ACS OMEGA

http://pubs.acs.org/journal/acsodf

Article

Synthesis of Fluorinated Hydrazinylthiazole Derivatives: A Virtual and Experimental Approach to Diabetes Management

Hasnain Mehmood, Tashfeen Akhtar,* Muhammad Haroon, Muhammad Khalid,* Simon Woodward, Muhammad Adnan Asghar, Rabia Baby, Raha Orfali,* and Shagufta Perveen

Cite This: *ACS Omega* 2023, 8, 11433−11446

Read Online

ACCESS | Metrics & More | Article Recommendations | Supporting Information

ABSTRACT: A novel series of fluorophenyl-based thiazoles was synthesized following the Hanztsch method. All of the compounds were initially verified with physical parameters (color, melting point, retardation factor (R_f)), which were further confirmed by several spectroscopic methods, including ultraviolet−visible (UV−visible), Fourier-transform infrared (FTIR), ^{1}H, ^{13}C, ^{19}F NMR, and high-resolution mass spectrometry (HRMS). The binding interactions of all compounds were studied using a molecular docking simulation approach. Furthermore, each compound was evaluated for its alpha(α)-amylase, antiglycation, and antioxidant potentials. The biocompatibility of all compounds was checked with an *in vitro* hemolytic assay. All synthesized scaffolds were found biocompatible with minimal lysis of human erythrocytes as compared to the standard Triton X-100. Among the tested compounds, the analogue **3h** (IC_{50} = 5.14 ± 0.03 μM) was found to be a highly potent candidate against α-amylase as compared to the standard (acarbose, IC_{50} = 5.55 ± 0.06 μM). The compounds **3d**, **3f**, **3i**, and **3k** exhibited excellent antiglycation inhibition potential with their IC_{50} values far less than the standard amino guanidine (IC_{50} = 0.403 ± 0.001 mg/mL). The antidiabetic potential was further supported by docking studies. Docking studies revealed that all synthesized compounds exhibited various interactions along enzyme active sites (pi−pi, H-bonding, van der Waals) with varied binding energies.

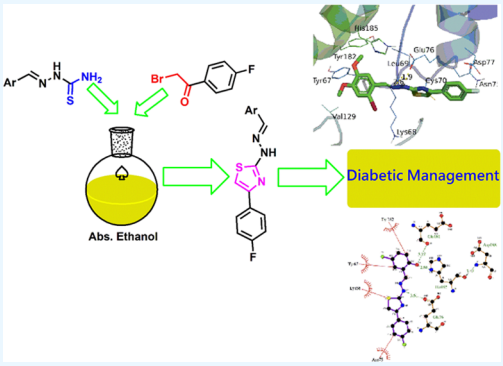

INTRODUCTION

Halogen tagged compounds have diverse distributions in nature and have a wide range of biological activities.[1−4] Besides natural distribution, synthetic halogen-substituted compounds hold a special place in medicinal chemistry. Their significance and regular use in medicinal chemistry is reinforced by the fact that, despite the COVID-19 pandemic, more than 20 drugs bearing halogen substituents have been approved by FDA for alternative clinical use (Figure 1).[5,6]

Due to the distinctive stability characteristics of halogens, lead optimization for drug development, frequently incorporates halogens within their core structures. Fluorine and chlorine are the most common substituents in this regard, as indicated in Figure 1. Thus, halo-organic variations are key frontiers of medicinal chemistry.[7] Their characteristic "halogen bonding"[8] renders their multitude of organic, inorganic, and biological systems.[9−12] The directional and strength comparability of halogen bonding with the hydrogen bond has attracted the widespread attention of medicinal chemists in medicinal chemistry.[13,14]

Fluorinated compounds do not show similar electrostatic potential trends to the other halogens due to small size of the fluorine atom.[12,15] Fluorine has weak ability to form halogen bonds, but its strong C−F bond facilitates tuning of the physicochemical properties and molecular conformations of the drug leads.[16] These properties include change in pK_a of neighboring functionalities,[17] lipophilicity,[18] enhanced membrane permeability,[19] and reduced steric effect.[20] The importance of fluorine in medicinal chemistry is further supported by the fact that 13 new drugs containing fluorine were approved by the FDA in 2022.[21] Some representative examples of these are presented in Figure 2.

The biological applications of halogenated compounds are also enriched when thiazole and hydrazinyl functionalities are also incorporated into their structures. Halogens in combination with hydrazinyl and thiazole moieties possess versatile biological activities.[22−28] Some important biological applications of halogenated hydrazinylthiazole compounds are shown in Figure 3.

Recently, Shahzadi et al. reported the antiglycation potential of alkyl-based hydrazinylthiazoles.[29] Compounds **I** and **II** (Figure 4) were highlighted as excellent antiglycating agents with IC_{50} values of 1.848 ± 0.646 and 0.0004 ± 1.097 μM,

Received: January 14, 2023
Accepted: March 7, 2023
Published: March 17, 2023

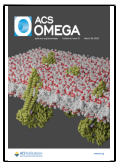

https://doi.org/10.1021/acsomega.3c00265
ACS Omega 2023, 8, 11433−11446

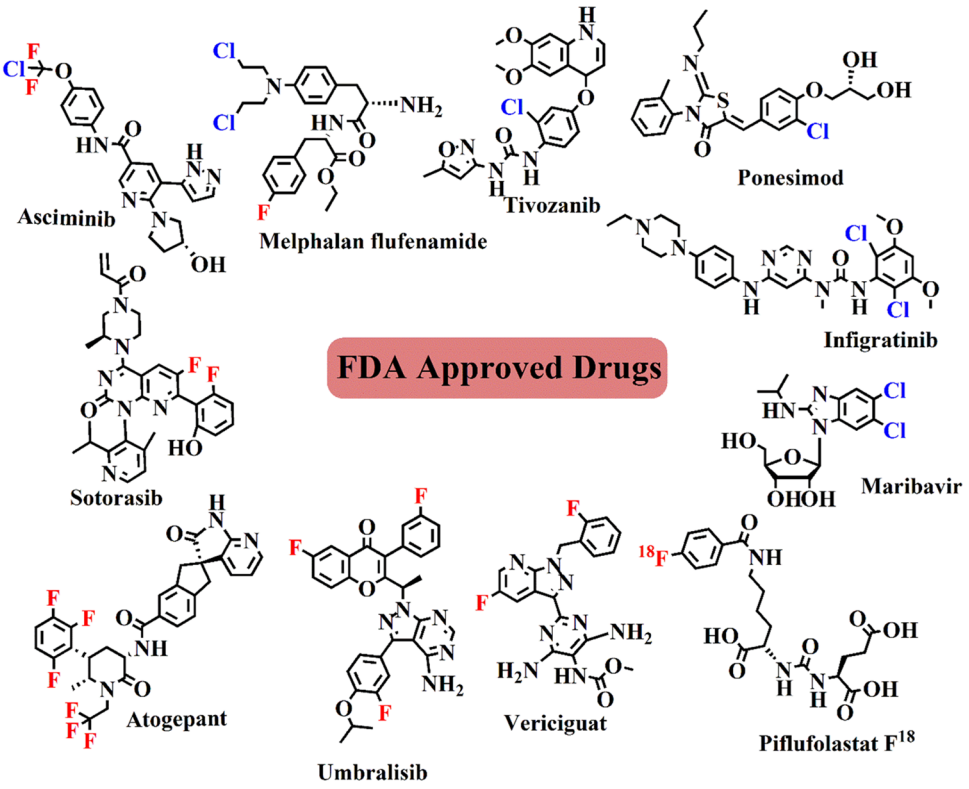

Figure 1. FDA-approved halogen-based drugs.

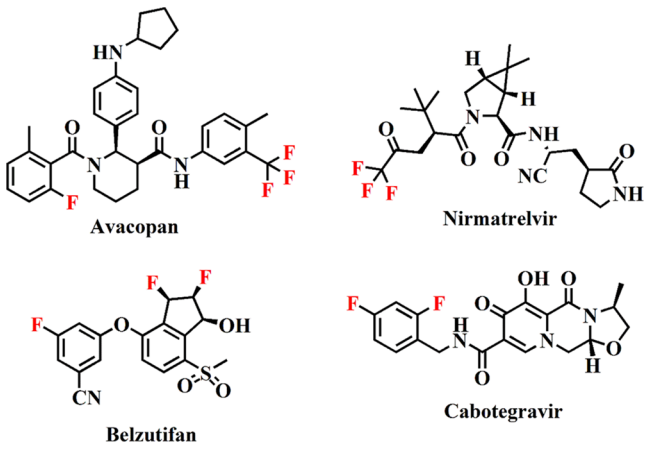

Figure 2. FDA-approved fluorine-containing drugs.

respectively (amino guanidine, IC_{50}= 25.50 ± 0.337 μM). In addition, Hasnain et al. reported the syntheses of two series of hydrazinylthiazoles and evaluated their antiglycation and α-amylase inhibition potential.[30,31] Compounds **III** and **IV** (Figure 4) were found to be potential α-amylase inhibitors with IC_{50} values of 4.80 ± 0.07 and 4.79 ± 0.08 μM, respectively (acarbose, IC_{50} = 5.62 ± 0.04 μM). They also reported compound **V** as an excellent antiglycating agent with IC_{50} value of 0.383 ± 0.001 mg/mL as compared to the standard amino guanidine (IC_{50} = 0.394 ± 0.001 mg/mL). The nonclassical bioisosterism, antidiabetic properties of halogenated compounds,[26,32−36] and in continuation of our research to explore thiazoles in search of an excellent antidiabetic agent guided us in structural planning of the proposed study (Figure 4).

RESULTS AND DISCUSSION

To synthesize 2-(2-arylidenehydrazinyl)-4-(4-fluorophenyl)-thiazoles (**3a−o**), an equimolar mixture of the respective thiosemicarbazones[30,31] (**1**) and 2-bromo-4-fluoroacetophenone (**2**) was condensed together under reflux in ethanol for 4−5 h, as shown in Scheme 1. Cyclized products were achieved in moderate to good yields (61−80%).

The formation of new compounds was clearly indicated by the change of physical parameters including color, melting points, and retardation factor (R_f) values. The structures of synthesized compounds were confirmed by spectroscopic studies (ultraviolet−visible (UV−visible), Fourier-transform infrared (FTIR), ^{1}H, ^{13}C and ^{19}F NMR) and mass spectral data. In the IR spectra of the compounds, characteristic absorption bands in the region 3278−3138 cm^{-1} were seen due to N−H stretching. The absorption stretchings in the range 3151−2933 cm^{-1} were attributed to aliphatic C−H functionality. Azomethine (−CH═N−) linkage was indicated by the characteristic of C═N stretching in the range of 1699−1600 cm^{-1}. Aromatic C═C stretching vibrations were observed in the region 1571−1436 cm^{-1}. Characteristic thiazole vibrations were interpreted for the absorption bands in the region 1068−692 cm^{-1}.[37]

In the ^{1}H NMR spectra of the synthesized compounds, the N−H group appears in the range 11.26−12.50 ppm and one proton singlet at 7.85−8.43 ppm was ascribed to the azomethine protons. The thiazole proton present at position 5 of the ring was observed at 6.22−7.50 ppm. The signals of all other aromatic and aliphatic protons were observed in their expected regions with multiplicities corresponding to the required substitution pattern of the ring.

In the ^{19}F NMR (proton-decoupled), one or two peaks corresponding to respective number of fluorine atoms present

https://doi.org/10.1021/acsomega.3c00265
ACS Omega 2023, 8, 11433−11446

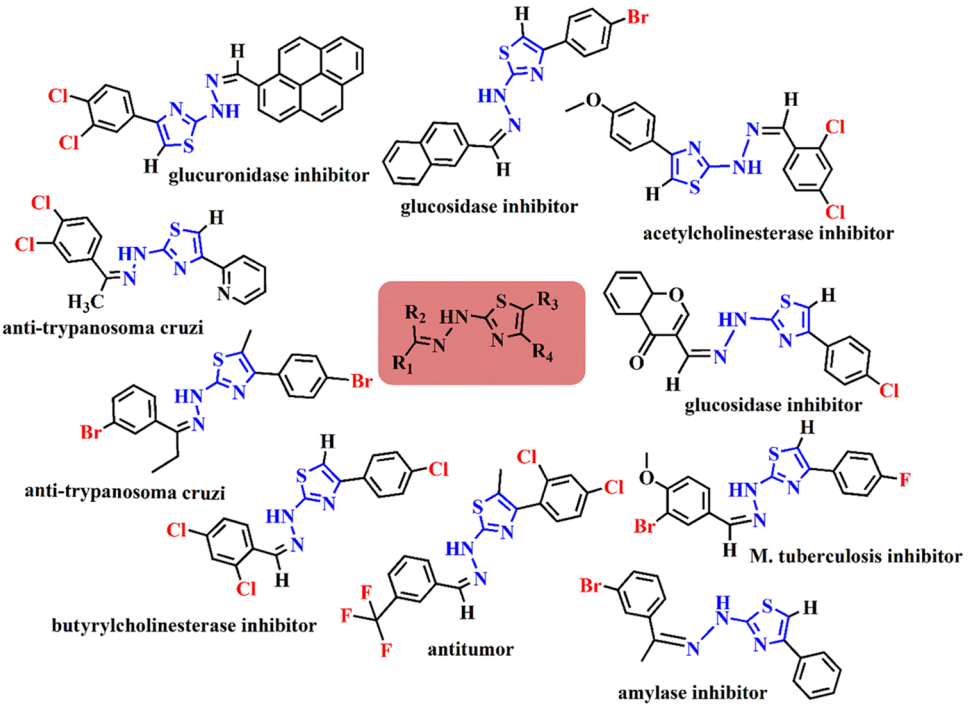

Figure 3. Biologically active halogenated hydrazinylthiazole-based scaffolds.

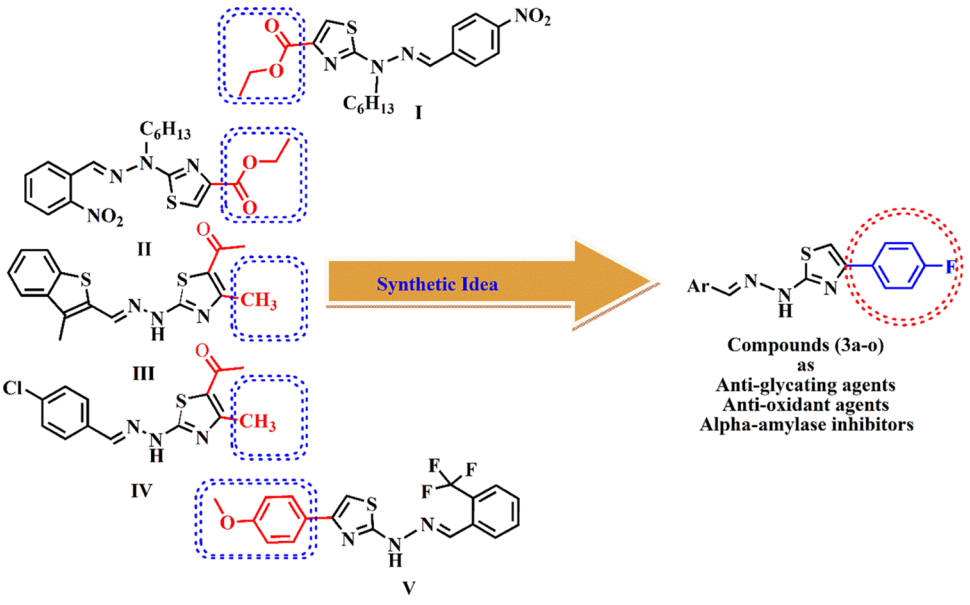

Figure 4. Synthetic inspiration for the targeted antidiabetic agents.

in the compounds were observed. For compounds **3d**, **3g**, **3i**, **3k**, and **3l**, two signals were observed, indicating two fluorine atoms present in the structure, while the remaining monofluorinated compounds gave a single signal in the region −114.49 to −114.77 ppm.

In the ^{13}C NMR spectra, signals of carbons at chemical shift values 168.3−170.6, 148.8−160.9, and 101.8−104.5 ppm were assigned to C2, C4, and C5 of the thiazole ring, respectively. The carbon of the azomethine linkage was indicated by a signal in the region 135.5−148.3 ppm. A characteristic doublet was observed for ipso carbons bonded with fluorine in the region 162.0−164.7 ppm with the coupling constant in the range of 244.3−249.4 ($^1J_{CF}$) Hz. Smaller doublets at 115.9−116.1 ppm were observed with the coupling constant $^2J_{CF}$ = 21.6 Hz. All other aromatic and aliphatic carbons were observed in their respective regions. The syntheses were further corroborated by high-resolution mass spectrometry (HRMS), where the calculated masses of synthesized compounds showed good agreement with the observed masses.

The synthesized compounds were assessed for their biological significance by evaluating the α-amylase, antiglycation, and antioxidant inhibition potentials. The cytotoxicity of all compounds was evaluated by *in vitro* hemolytic activity.

Biological Screening of 2-(2-Arylidenehydrazinyl)-4-(4-fluorophenyl)thiazoles (3a−o) α-Amylase Inhibition Activity. The compounds (**3a−o**) were evaluated for their

https://doi.org/10.1021/acsomega.3c00265
ACS Omega 2023, 8, 11433−11446

Scheme 1. : Synthesis of 2-(2-Arylidenehydrazinyl)-4-(4-fluorophenyl)thiazoles (3a−o)

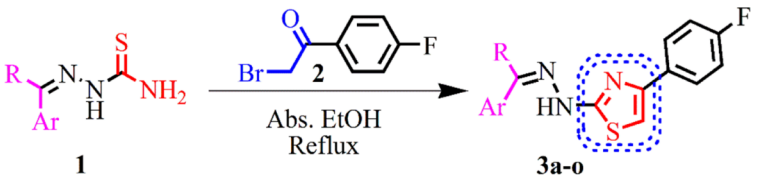

Compd.	−Ar	-R	Compd.	−Ar	-R
3a	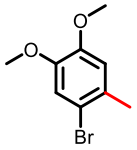	-H	3i	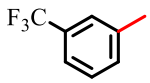	-H
3b	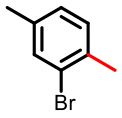	-H	3j	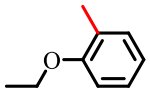	-H
3c	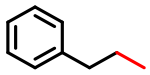	-CH_3	3k	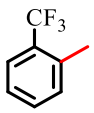	-H
3d	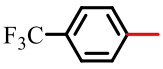	-H	3l	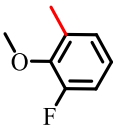	-H
3e	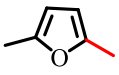	-H	3m		-H
3f	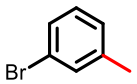	-CH_3	3n		-H
3g	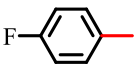	-CH_3	3o	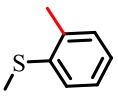	-H
3h	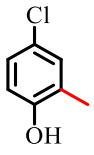	-H			

enzyme inhibition potential against α-amylase, and the results are presented in Table 1. Acarbose was used as the standard (reference inhibitor) with an IC_{50} value of 5.55 ± 0.06 μM. All tested compounds exhibited enzyme inhibition potency from moderate to high with an effect of concentration. The IC_{50} values revealed that their inhibition potential is dose-dependent. The compound **3h** (5-chloro-2-hydroxy) was found to be a more potent (IC_{50}= 5.14 ± 0.03 μM) α-amylase inhibitor when compared with the standard. Besides **3h**, the compound **3n** (thiophen-2-yl, IC_{50}= 5.77 ± 0.05 μM) showed good enzyme inhibition compared to the standard.

Similarly, the IC_{50} values of compounds **3b** (2-bromo-4-methyl, IC_{50}= 6.87 ± 0.01 μM) and **3f** (3-bromo, IC_{50}= 5.88 ± 0.16 μM) indicated that they also have almost comparable enzyme inhibition potential to the standard. The structure−activity relationship (SAR) studies revealed that the compound **3h**, containing the −OH group, enhances the ability of the compound to form strong hydrogen bonding with the enzyme. The reason for exhibiting the comparable inhibition potential may be because of having the same substituent at different positions, which may be related to compounds **3d**, **3i**, and **3k** showing a similar behavior.

Antiglycation Activity. The synthesized compounds (**3a−o**) were further evaluated for their antiglycation potential using amino guanidine as the reference inhibitor (IC_{50}= 0.403 ± 0.001 mg/mL) as shown in Table 2. All compounds possess good to excellent antiglycation potential, with IC_{50} values ranging from 0.393 ± 0.002 to 0.584 ± 0.006 mg/mL.

An initial SAR was established for targeted compounds, which indicated that the inhibition potential depends upon the nature of the substituent and its position on the aromatic ring. Compound **3i** exhibited the highest inhibition activity (IC_{50}= 0.393 ± 0.002 mg/mL) having the trifluoromethyl group at position 3. Compounds **3d** and **3k** were also found to be more potent than the standard having IC_{50} values of 0.394 ± 0.003 and 0.396 ± 0.002 mg/mL, respectively. The comparable

https://doi.org/10.1021/acsomega.3c00265
ACS Omega 2023, 8, 11433−11446

Table 1. Percentage α-Amylase Inhibition along with IC_{50} Values of Compounds 3a−o

	% age α-amylase inhibition			
compd.	1 μM	5 μM	10 μM	IC_{50} ± SEM (μM)
3a	35.96	51.11	69.11	6.41 ± 0.09
3b	31.95	51.54	62.71	6.87 ± 0.01
3c	30.03	45.41	58.12	7.52 ± 0.05
3d	36.97	49.93	62.35	6.92 ± 0.12
3e	30.06	41.20	57.45	7.77 ± 0.01
3f	34.92	51.68	62.28	6.88 ± 0.16
3g	38.00	49.56	62.75	6.90 ± 0.23
3h	55.89	69.05	82.47	5.14 ± 0.03
3i	38.90	51.09	64.58	6.70 ± 0.08
3j	29.58	42.23	54.03	8.07 ± 0.12
3k	47.84	57.72	70.90	6.03 ± 0.04
3l	37.06	49.08	61.72	7.00 ± 0.13
3m	42.76	52.79	63.94	6.66 ± 0.13
3n	51.64	64.48	71.83	5.77 ± 0.05
3o	33.07	43.03	57.18	7.69 ± 0.18
acarbose	53.42	66.81	74.77	5.55 ± 0.06

antiglycation potential of compounds **3d**, **3i**, and **3k** is ascribed to the presence of the same substituent (trifluoromethyl) at positions 4, 3, and 2, respectively. The compound **3f** bearing the bromine atom at position 3 also exhibited more antiglycation potential (IC_{50}= 0.399 ± 0.002 mg/mL), compared to the standard. The IC_{50} values of all other tested compounds indicated that the inhibitory potential depends upon the substituent on the aromatic ring. The results also revealed that the percentage antiglycation is also dose-dependent; with an increase in concentration of the tested sample, the antiglycation activity increases.

SAR studies also revealed that the antiglycation activity is affected by the nature of groups present around the thiazole ring. While comparing our current results with previous studies, it may be concluded that the presence of 4-fluorophenyl functionality around the thiazole ring enhanced the glycation inhibition potential of the compounds. The argument may be strengthened by the current results, where **3k**, **3i**, and **3d** showed enhanced antiglycation activity as compared to the standard (Figure 5).[30,31]

Free Radical Scavenging Ability (Antioxidant Activity). The compounds **3a−o** were screened for their DPPH free radical scavenging ability, and the results are presented in Table 3. Most compounds showed fairly good antioxidant potential but less active than the standard (IC_{50} = 7.18 ± 0.01 mM). The compound **3j**, bearing the ethoxy group at position 2 of the arylidene ring, was found to be the most active in this series with an IC_{50} value of 8.33 ± 0.08 mM, almost comparable to that of the standard. The increased percentage antioxidant potential of the other compounds is as follows: **3o** < **3n** < **3l** < **3a** < **3c** < **3b** < **3d**. The percentage antioxidant potential of the other compounds **3e**, **3f**, **3g**, **3h**, **3i**, **3k**, and **3m** was less than 50%, so their IC_{50} values were not calculated. The results revealed that the percentage antioxidant potential is also dose-dependent. Most of the tested compounds at their lower concentration did not show significant activity but were found to be active when the concentration increases.

***In Vitro* Hemolytic Activity.** The compounds **3a−o** were screened for their cytotoxicity behavior through a hemolytic assay, and the results are presented in Table 4. The compounds **3b**, **3c**, **3f**, **3j**, and **3l** were found safe at their minimum treated concentration (10 μM), while all other compounds were found to be fatal to red blood cells and caused lysis of RBCs at all tested concentrations. The percentage hemolysis is also found to be dose-dependent; lysis increases when the concentration of the sample increases.

Molecular Docking. The compounds **3a−o** were virtually screened against two proteins, *i.e.*, human serum albumin (HSA) and human pancreatic α-amylase (HPA), by molecular docking. HSA is a carrier protein that also serves as a marker for uncontrolled diabetes. This protein becomes heavily glycated due to long-term elevated glucose levels.[38] The protein glycation may contribute to oxidative stress and inflammation. Here, we have performed antiglycation studies for the synthesized ligands (**3a−o**) using the HSA three-dimensional structure as a target protein. HAS has multiple glycation sites (F1−9) in its three domains.[39,40] Sudlow site II is a fatty acid binding site mainly consisting of Leu^{115}, Pro^{118}, Met^{123}, Ala^{126}, Phe^{134}, Lys^{137}, Tyr^{138}, Glu^{141}, Ile^{142}, His^{146},

Table 2. Percentage Antiglycation Inhibition along with IC_{50} Values of Compounds 3a−o

	% age antiglycation inhibition						
compd.	100 ppm	200 ppm	400 ppm	600 ppm	800 ppm	1000 ppm	IC_{50} (mg ± SEM)
3a	80.912	82.097	84.808	85.864	86.983	89.880	0.410 ± 0.003
3b	81.189	84.602	85.170	86.200	86.768	87.462	0.413 ± 0.002
3c	67.583	68.855	69.669	75.722	77.932	81.626	0.464 ± 0.002
3d	87.417	87.923	89.045	89.475	90.859	92.275	0.394 ± 0.003
3e	68.735	69.659	70.703	71.831	72.794	73.677	0.493 ± 0.003
3f	84.146	86.734	87.272	87.994	90.418	91.338	0.399 ± 0.002
3g	24.260	34.557	48.804	54.331	66.643	74.646	0.584 ± 0.006
3h	50.878	56.497	65.488	68.424	68.964	70.744	0.528 ± 0.002
3i	87.964	88.535	89.110	89.990	91.164	92.228	0.393 ± 0.002
3j	52.257	61.537	66.470	70.267	76.184	79.161	0.488 ± 0.003
3k	87.393	87.943	88.776	89.221	89.978	91.580	0.396 ± 0.002
3l	79.853	81.769	83.050	84.648	86.160	87.099	0.418 ± 0.005
3m	76.769	78.789	82.499	83.963	86.080	88.774	0.418 ± 0.002
3n	79.297	80.987	82.086	83.014	85.776	87.827	0.420 ± 0.003
3o	83.693	84.223	85.521	86.434	88.18	89.496	0.407 ± 0.002
amino guanidine	85.190	86.141	87.143	88.011	88.866	89.657	0.403 ± 0.001

https://doi.org/10.1021/acsomega.3c00265
ACS Omega 2023, 8, 11433−11446

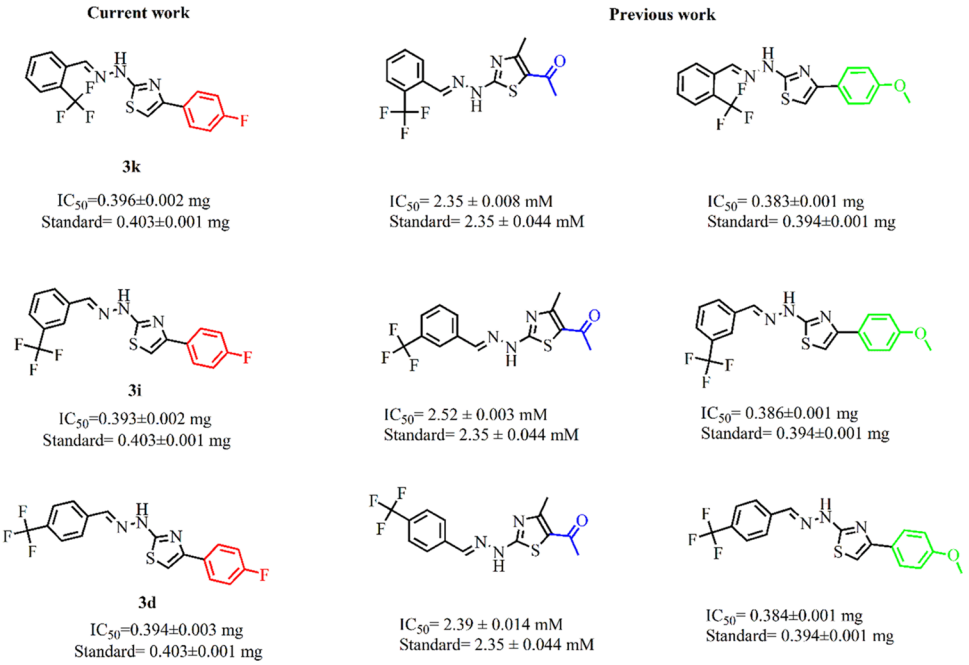

Figure 5. Antiglycation activity: structural comparison of our current work with previously reported work.

Table 3. Percentage Antioxidant Potential along with IC_{50} Values of Compounds 3a−o[a]

	% age antioxidant potential					
compd.	3 mM	6 mM	9 mM	12 mM	15 mM	IC_{50} (mM ± SEM)
3a	0.00	18.82	32.72	47.58	67.95	12.39 ± 0.10
3b	8.77	23.69	36.38	53.65	69.82	11.32 ± 0.14
3c	0.00	11.13	34.28	57.51	73.34	11.43 ± 0.12
3d	23.48	34.45	45.32	56.39	63.78	10.68 ± 0.08
3e	0.00	8.26	19.32	44.74	49.04	
3f	0.00	0.00	19.48	28.70	40.73	
3g	0.00	0.00	0.00	0.00	8.45	
3h	0.00	0.00	0.00	8.78	23.25	
3i	0.00	8.64	18.87	32.26	46.53	
3j	18.18	45.90	62.07	75.45	78.51	8.33 ± 0.08
3k	0.00	14.08	21.05	30.92	48.28	
3l	0.00	15.62	32.06	46.14	65.18	12.94 ± 0.01
3m	0.00	0.00	0.00	15.13	31.05	
3n	0.00	12.72	30.39	45.47	59.36	13.86 ± 0.04
3o	0.00	7.68	18.22	30.15	53.73	17.97 ± 0.27
ascorbic acid	52.34	61.01	74.41	81.85	84.92	7.18 ± 0.01

[a]IC_{50} values: Concentration of the sample (mM) at which DPPH is scavenged by 50%.

Phe[149], Leu[154], Phe[157], Tyr[161], Leu[185], Arg[186], Gly[189], Lys[190], and Ser[193] amino acids. The ligand **3a** shows binding to the same Sudlow site II with a binding energy of −9.54 kcal/mol and a binding constant of 102 nM (Table 5). In the same site, two lysines and one histidine amino acid, i.e., Lys[137], His[146], and Lys[190], constitute a major glycation site (FA1) in domain IB.[41] The ligands **3**(**d**, **f**, **i**, and **k**) share the same binding site involving Lys[137], Leu[115], Arg[117], Met[123], Ala[126], Phe[127], Asp[129], Asn[130], Thr[133], Phe[134], Lys[137], Tyr[138], Glu[141], Ile[142], Tyr[161], Phe[165], and Leu[182] residues (Figure 6). These ligands form $\pi-\pi$ stacking interactions with Tyr[138] and show interactions with Lys[137], one of the main residues that undergo glycation.[42] Tyr[138] and Tyr[161] have previously been reported to interact with macrocycle rings of various drugs by $\pi-\pi$ stacking,[43] while Tyr[161] and His[146] are involved in the heme−Fe atom coordination; any ligand binding to these sites may disrupt heme−Fe interactions.[41] Among these ligands, **3f** shows a binding energy of −9.22 kcal/mol and a dissociation constant of 173 nM (Table 5). Although **3h** shows a binding constant of 223 nM and a binding energy of −9.07 kcal/mol, it binds to a shared region of Sudlow sites I and II comprising residues, i.e., Ala[191], Lys[195], Leu[198], Lys[199], Ser[202], Ala[210], Phe[211], Trp[214], Lys[436], Pro[447], Cys[448], Ala[449], Asp[451], Tyr[452], Val[455], and Leu[481]. This binding site includes a part of Sudlow site I, where Lys[199] is responsible for 5% of the total glycation.[44,45] *In vitro* results also corroborate the best IC_{50} obtained with the same ligands exhibiting the highest binding energy in the *in silico* studies. Previously, triazole-based Schiff bases and thiazole-based thiosemicarbazones had shown antiglycation activities by *in silico* studies.[46]

Human pancreatic α-amylase (HPA) has multiple ligand binding sites in its three-domain structure.[47,48] Ligands **3a**−**o**

https://doi.org/10.1021/acsomega.3c00265
ACS Omega 2023, 8, 11433−11446

Table 4. Percentage Hemolysis of Compounds 3a−o

compd.	% hemolysis		
	10 μM	50 μM	100 μM
3a	3.06	15.10	32.23
3b	0.00	7.90	31.56
3c	0.00	8.38	32.09
3d	16.05	25.71	40.97
3e	1.20	11.50	40.38
3f	0.00	15.57	40.19
3g	1.98	26.35	52.27
3h	3.11	21.17	52.50
3i	14.70	30.72	44.54
3j	0.00	16.83	32.47
3k	4.43	27.62	45.69
3l	0.00	19.99	36.64
3m	2.58	26.29	46.22
3n	11.42	32.43	61.41
3o	1.99	21.55	49.12
triton X-100	100	100	100

have been found to interact in four of these sites, with the binding energies ranging from −8.78 to −7.22 kcal/mol (Table 6). In HPA, Trp,[59] Asp^{197}, and Glu^{233} are the main catalytic site amino acids that interact with α-amylase inhibitors *via* π−π stacking, van der Waals, and H-bonding interactions, respectively. Many natural and synthetic compounds have been found to interact with active site residues (Trp^{59}, Asp^{197}, and Glu^{233}) in HPA.[49−51] In our study, most of the ligands, i.e., **3(a, c, e, i−o)**, were found to interact with these active site residues (Figure 7). The ligand **3a** was found to be a better α-amylase inhibitor. It interacts with all three domains of HPA while binding at four different sites (Figure 7). The ligand **3a** shows the best binding energy (−8.59 kcal/mol) with a dissociation constant of ∼506 nM when interacting with the C-terminal domain (Domain III) and −7.94 kcal/mol of binding energy with 1.5 μM dissociation constant when binding to the main active site of the enzyme (Table 6). The active site residues include Trp^{58}, Trp^{59}, Tyr^{62}, Gln^{63}, His^{101}, Gly^{104}, Asn^{105}, Ala^{106}, Val^{107}, Leu^{162}, Thr^{163}, Gly^{164}, Leu^{165}, Arg^{195}, Asp^{197}, Ala^{198}, Glu^{233}, His^{299}, and Asp^{300} (Figure 7). Here, $Ala,^{105,106}$ Gln^{63}, and Arg^{195} are found to interact *via* H-bonding. *In silico* findings for ligand **3n** agree with the *in vitro* results. It interacts proximate to the active site residues with a binding energy of −8.31 kcal/mol and a dissociation constant of 8.1 μM (Table 6). The ligand **3h**, which has been found to be the best α-amylase inhibitor in experimental IC_{50}, interacts proximate to N- and C-terminal domains and does not directly disrupt the enzyme active site (Figure 7). The ligand **3k** interacts with active site residues (Trp^{59}, Glu^{60}, Tyr^{62}, Gln^{63}, His^{101}, Tyr^{151}, Leu^{162}, Thr^{163}, Leu^{165}, Asp^{197}, Ala^{198}, Ser^{199}, Lys^{200}, His^{201}, Glu^{233}, Val^{234}, Ile^{235}) as well as domain III (C-terminal) of the enzyme with binding energies of -7.76 and -7.71 kcal/mol with dissociation constants of 2.06 and 2.23 μM (Table 6). The ligand **3k** also showed an IC_{50} of 6.03 ± 0.04 μM in *in vitro* amylase inhibition (Table 1). Previously, some α-amylase inhibitors were found to form hydrogen bonds with Ile^{235} and Glu^{233} and charge−π interactions with His^{151}. In our findings, His^{101} and His^{201} have been found to interact with **3a−o** ligands *via* charge−π and π−π interactions.

CONCLUSIONS

The current study was carried out for the synthesis of fluorophenyl-based hydrazinylthiazole derivatives. 15 compounds were synthesized through a two-step synthetic protocol, and the majority of the compounds were obtained in good yields. The verification of formation and confirmation of the proposed skeleton of all synthesized scaffolds was achieved with spectroscopic techniques (UV−visible, FTIR, ^{1}H, ^{13}C, ^{19}F NMR, HRMS). Biological screening of all synthesized compounds was carried out against α-amylase, glycation, and oxidation processes. The synthesized compounds showed comparable with standard to excellent activities. The compound **3h** was found to be an excellent α-

Table 5. *In Silico* Antiglycation Activity with Binding Energy and Dissociation Constant of All Compounds 3a−o

ligands	binding energy (kcal/mol)	dissociation constant (nM)	active site
3a	−9.54	102.28	Leu^{115}, Pro^{118}, Met^{123}, Ala^{126}, Phe^{134}, Lys^{137}, Tyr^{138}, Glu^{141}, Ile^{142}, His^{146}, Phe^{149}, Leu^{154}, Phe^{157}, Tyr^{161}, Leu^{185}, Arg^{186}, Gly^{189}, Lys^{190}, Ser^{193}.
3b	−8.64	465.05	Leu^{115}, Met^{123}, Ala^{126}, Phe^{127}, Asp^{129}, Asn^{130}, Thr^{133}, Phe^{134}, Lys^{137}, Tyr^{138}, Glu^{141}, Ile^{142}, Tyr^{161}.
3c	−9.09	216.92	Leu^{115}, Val^{116}, Arg^{117}, Pro^{118}, Met^{123}, Phe^{134}, Lys^{137}, Tyr^{138}, Glu^{141}, Ile^{142}, His^{146}, Phe^{149}, Phe^{157}, Tyr^{161}, Phe^{165}, Leu^{182}, Leu^{185}, Arg^{186}, Gly^{189}, Lys^{190}.
3d	−8.53	557.19	Leu^{115}, Met^{123}, Ala^{126}, Phe^{127}, Asp^{129}, Asn^{130}, Glu^{131}, Thr^{133}, Phe^{134}, Lys^{137}, Tyr^{138}, Glu^{141}, Ile^{142}, Tyr^{161}.
3e	−8.64	462.69	Leu^{115}, Met^{123}, Ala^{126}, Phe^{127}, Asp^{129}, Asn^{130}, Glu^{131}, Thr^{133}, Phe^{134}, Lys^{137}, Tyr^{138}, Glu^{141}, Ile^{142}, Tyr^{161}.
3f	−9.22	173.72	Leu^{115}, Pro^{118}, Met^{123}, Phe^{134}, Lys^{137}, Tyr^{138}, Glu^{141}, Ile^{142}, His^{146}, Tyr^{161}, Leu^{182}, Leu^{185}, Arg^{186}, Gly^{189}, Lys^{190}.
3g	−8.7	421.72	Leu^{115}, Pro^{118}, Met^{123}, Phe^{134}, Lys^{137}, Tyr^{138}, Glu^{141}, Ile^{142}, His^{146}, Phe^{149}, Tyr^{161}, Leu^{182}, Leu^{185}, Arg^{186}, Gly^{189}, Lys^{190}.
3h	−9.07	223.24	Ala^{191}, Lys^{195}, Leu^{198}, Lys^{199}, Ser^{202}, Ala^{210}, Phe^{211}, Trp^{214}, Lys^{436}, Pro^{447}, Cys^{448}, Ala^{449}, Asp^{451}, Tyr^{452}, Val^{455}, Leu^{481}.
3i	−8.65	457.99	Leu^{115}, Arg^{117}, Met^{123}, Ala^{126}, Phe^{127}, Asp^{129}, Asn^{130}, Thr^{133}, Phe^{134}, Lys^{137}, Tyr^{138}, Glu^{141}, Ile^{142}, Tyr^{161}, Leu^{182}.
3j	−8.62	484.08	Leu^{115}, Arg^{117}, Met^{123}, Ala^{126}, Phe^{127}, Asp^{129}, Asn^{130}, Thr^{133}, Phe^{134}, Lys^{137}, Tyr^{138}, Glu^{141}, Ile^{142}, Tyr^{161}, Phe^{165}, Leu^{182}.
3k	−8.53	560.99	Leu^{115}, Arg^{117}, Met^{123}, Ala^{126}, Phe^{127}, Asp^{129}, Asn^{130}, Thr^{133}, Phe^{134}, Lys^{137}, Tyr^{138}, Glu^{141}, Ile^{142}, Tyr^{161}, Phe^{165}, Leu^{182}.
3l	−9.1	212.44	Leu^{115}, Arg^{117}, Met^{123}, Lys^{137}, Tyr^{138}, Glu^{141}, Ile^{142}, His^{146}, Phe^{149}, Leu^{154}, Phe^{157}, Tyr^{161}, Phe^{165}, Leu^{182}, Leu^{185}, Arg^{186}, Gly^{189}, Lys^{190}, Ser^{193}.
3m	−8.33	786.45	Leu^{115}, Met^{123}, Ala^{126}, Phe^{127}, Asp^{129}, Asn^{130}, Glu^{131}, Thr^{133}, Phe^{134}, Lys^{137}, Tyr^{138}, Glu^{141}, Ile^{142}, Tyr^{161}.
3n	−8.19	1000.00	Leu^{115}, Met^{123}, Ala^{126}, Phe^{127}, Asp^{129}, Asn^{130}, Thr^{133}, Phe^{134}, Lys^{137}, Tyr^{138}, Glu^{141}, Ile^{142}, Tyr^{161}.
3o	−8.51	578.33	Leu^{115}, Arg^{117}, Met^{123}, Ala^{126}, Phe^{127}, Asp^{129}, Asn^{130}, Thr^{133}, Phe^{134}, Lys^{137}, Tyr^{138}, Glu^{141}, Ile^{142}, Tyr^{161}, Phe^{165}, Leu^{182}.

https://doi.org/10.1021/acsomega.3c00265
ACS Omega 2023, 8, 11433−11446

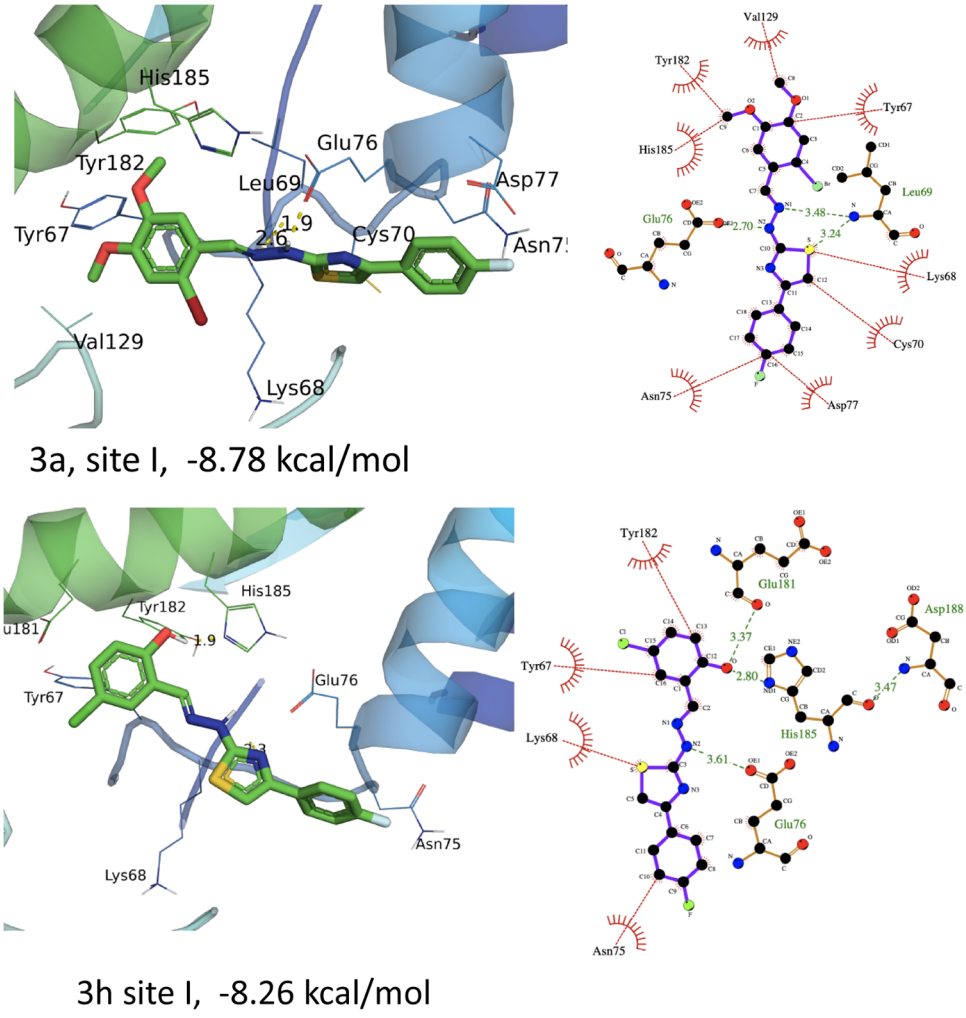

Figure 6. Best docking interactions are shown by ligands **3a** and **3h** with binding energies of −8.78 and −8.26 kj/mol against human pancreatic α-amylase (HPA).

amylase inhibitor. The compounds **3d**, **3f**, **3i**, and **3k** showed the highest potency for the glycation inhibition process. All synthesized scaffolds were found biocompatible in nature due to minimal lysis of human erythrocytes as compared to the standard Triton X-100. All synthesized compounds exhibited various interactions along enzyme active sites (pi−pi, H-bonding, van der Waals) with varied binding energies evaluated through a molecular docking study.

EXPERIMENTAL SECTION

Materials and Methods. All reagents and solvents used in syntheses of compounds **3a**−**o** were of analytical grade and used as received without further purification. The reagents and solvents were purchased from commercial sources (Sigma-Aldrich Merck, Fischer, and Acros Organics). Precoated thin-layer chromatographic aluminum sheets (Kiesel gel 60, F_{254}, E. Merck, Germany) were used to monitor the progress and purity of synthesized compounds. Melting points (M.p.) were recorded in open capillaries using a DMP-300 A&E Lab, U.K., melting point apparatus and are uncorrected. Ultraviolet (UV) absorption spectra were recorded on a Shimadzu Ultraviolet-1800 spectrophotometer in DMSO. IR spectra were recorded on a Bruker OPUS using attenuated total reflectance (ATR) to identify the functional groups. Proton (^{1}H), carbon (^{13}C), and fluorine (^{19}F) NMR experiments were performed on Bruker DPX-400 and 500 MHz spectrometers. Mass spectra were recorded on the Bruker Micro time of flight-electrospray ionization (TOF-ESI) positive targeted mode. Fluorescence of glycated products was measured on a Shimadzu RF-6000 spectrofluorometer.

*General Procedure for the Syntheses of 2-(2-Arylidenehydrazinyl)-4-(4-fluorophenyl)thiazoles (**3a**−**o**).* The synthesis of **3a**−**o** was achieved by the Hantzsch thiazole synthetic protocol. Respective aryl-substituted thiosemicarbzones[30,31] (0.001 mol) and 2-bromo-4-fluoroacetophenone (0.001 mol) in absolute ethanol were heated under reflux for 4−5 h. Reaction progress and completion were indicated by TLC, measured at regular intervals. Appearance of a single spot on the TLC plate highlighted the completion of reaction. Upon completion, the reaction mixture was allowed to attain room temperature for 30 min. The reaction mixture was then poured on crushed ice, which resulted in precipitation of the solid. The resulting precipitated solid was filtered through suction. The obtained solid was washed with plenty of water to remove the mother liquor. The formed solid was dried under vacuum to obtain the pure product. The NMR spectra (400 MHz) of **3a**−**o** were recorded in $DMSO_{d_6}$ except for **3a**, **3c**, and **3d**, which were run in chloroform $CDCl_3$.

*2-(2-(2-Bromo-4,5-dimethoxybenzylidene)hydrazinyl)-4-(4-fluorophenyl)thiazole (**3a**).* Brick-red solid; yield: 79%;

https://doi.org/10.1021/acsomega.3c00265
ACS Omega 2023, 8, 11433−11446

Table 6. *In Silico* α-Amylase Inhibition Potential with Binding Energy and Dissociation Constant of All Compounds 3a−o

ligands	binding energy (kcal/mol)	dissociation constant (μM)	active site
3a	−8.78	0.36	Tyr^{2}, Ser^{3}, Asn^{5}, Thr^{6}, Gln^{7}, Gln^{8}, Arg^{92}, Leu^{217}, Trp^{221}, Phe^{222}, Pro^{223}, Gly^{225}, Ser^{226}, Lys^{227}, Pro^{228}, Phe^{229}, Ile^{230}.
3a	−8.59	0.51	Asp^{451}, Ile^{453}, Ser^{454}, Ile^{465}, Lys^{466}, Ile^{467}, Tyr^{468}, Ala^{475}, His^{476}, Phe^{477}, Ser^{478}, Ile^{479}, Ser^{480}, Ala^{483}, Glu^{484}, Asp^{485}, Phe^{487}, Ile^{488}.
3a	−7.94	1.52	Trp^{58}, Trp^{59}, Tyr^{62}, Gln^{63}, His^{101}, Gly^{104}, Asn^{105}, Ala^{106}, Val^{107}, Leu^{162}, Thr^{163}, Gly^{164}, Leu^{165}, Arg^{195}, Asp^{197}, Ala^{198}, Glu^{233}, His^{299}, Asp^{300}.
3a	−7.89	1.64	Tyr^{67}, Lys^{68}, Leu^{69}, Cys^{70}, Asn^{75}, Glu^{76}, Asp^{77}, Cys^{115}, Lys^{178}, Glu^{181}, Tyr^{182}, His^{185}, Leu^{186}.
3b	−7.91	1.6	Thr^{439}, Ile^{465}, Lys^{466}, Ile^{467}, Tyr^{468}, Ser^{470}, Asp^{472}, Lys^{474}, Ala^{475}, His^{476}, Phe^{477}, Ser^{478}, Ile^{488}.
3b	−7.74	2.12	Arg^{267}, Gln^{302}, Arg^{303}, Gly^{304}, His^{305}, Ala^{310}, Ile^{312}, Thr^{314}, Trp^{316}, Asp^{317}, Arg^{346}, Phe^{348}, Gly^{351}, Asn^{352}, Asp^{353}, Val^{354}, Asp^{356}.
3c	−8.1	1.16	Trp^{59}, Tyr^{62}, Gln^{63}, His^{101}, Tyr^{151}, Leu^{162}, Thr^{163}, Leu^{165}, Arg^{195}, Asp^{197}, Ala^{198}, Ser^{199}, Lys^{200}, His^{201}, Glu^{233}, Val^{234}, Ile^{235}.
3c	−7.62	2.59	Arg^{389}, Gln^{390}, Asp^{451}, Ile^{453}, Ser^{454}, Ile^{465}, Lys^{466}, Ile^{467}, Tyr^{468}, His^{476}, Phe^{477}, Ser^{478}, Ile^{479}, Ser^{480}, Ala^{483}, Glu^{484}, Asp^{485}, Pro^{486}, Phe^{487}, Ile^{488}.
3d	−7.61	2.65	Tyr^{67}, Lys^{68}, Leu^{69}, Cys^{70}, Asn^{75}, Glu^{76}, Asp^{77}, Cys^{115}, Ala^{128}, Val^{129}, Lys^{178}, Glu^{181}, Tyr^{182}, His^{185}.
3e	−7.3	4.44	Tyr 67, Lys 68, Leu 69, Cys 70, Asn 75, Glu 76, Asp 77, Cys 115, Ala 128, Val 129, Lys 178, Glu 181, Tyr 182, His 185
3e	−7.22	5.07	Arg 389, Gln 390, Ser 435, Phe 436, Ser 437, Asp 451, Ile 453, Ser 454, Ile 465, Ser 478, Ile 479, Ser 480, Ala 483, Glu 484, Asp 485, Pro 486, Phe 487, Ile 488
3f	−7.83	1.83	Arg 389, Ser 435, Phe 436, Ser 437, Asp 451, Ile 453, Ser 454, Ile 465, Ser 478, Ile 479, Ser 480, Ala 483, Glu 484, Asp 485, Pro 486, Phe 487, Ile 488
3f	−7.78	2.00	Ser 66, Tyr 67, Lys 68, Leu 69, Cys 70, Asn 75, Glu 76, Asp 77, Cys 115, Ala 128, Val 129, Glu 181, Tyr 182, His 185
3g	−7.42	3.66	Arg 389, Gln 390, Ser 435, Phe 436, Ser 437, Asp 451, Ile 453, Ser 454, Ile 465, Ser 478, Ile 479, Ser 480, Ala 483, Glu 484, Asp 485, Pro 486, Phe 487, Ile 488
3h	−8.26	0.88	Tyr 67, Lys 68, Leu 69, Cys 70, Asn 75, Glu 76, Asp 77, Cys 115, Ala 128, Val 129, Lys 178, Glu 181, Tyr 182, His 185
3h	−8.18	1.01	Thr 439, Ile 465, Lys 466, Ile 467, Tyr 468, Ser 470, Lys 474, Ala 475, His 476, Phe 477, Ser 478, Ile 488
3i	−7.99	1.40	Ser 66, Tyr 67, Lys 68, Leu 69, Cys 70, Asn 75, Glu 76, Asp 77, Cys 115, Ala 128, Val 129, Glu 181, Tyr 182, His 185
3j	−7.74	2.12	Asp 451, Ile 453, Ser 454, Ile 465, Lys 466, Ile 467, Tyr 468, Ala 475, His 476, Phe 477, Ser 478, Ile 479, Ser 480, Ala 483, Glu 484, Asp 485, Pro 486, Phe 487, Ile 488
3j	−7.51	3.11	Trp 59, Glu 60, Tyr 62, Gln 63, His 101, Tyr 151, Leu 162, Thr 163, Leu 165, Asp 197, Ala 198, Ser 199, Lys 200, His 201, Glu 233, Val 234, Ile 235
3k	−7.76	2.06	Trp 59, Glu 60, Tyr 62, Gln 63, His 101, Tyr 151, Leu 162, Thr 163, Leu 165, Asp 197, Ala 198, Ser 199, Lys 200, His 201, Glu 233, Val 234, Ile 235
3k	−7.71	2.23	Thr 439, Ile 465, Lys 466, Ile 467, Tyr 468, Ser 470, Asp 472, Lys 474, Ala 475, His 476, Phe 477, Ser 478, Ile 488
3l	−8.31	0.80	Trp 58, Trp 59, Tyr 62, His 101, Tyr 151, Leu 162, Leu 165, Arg 195, Asp 197, Ala 198, Ser 199, Lys 200, His 201, Glu 233, Val 234, Ile 235, Glu 240, Asn 298, His 299, Asp 300
3m	−7.61	2.65	Arg 267, Gln 302, Arg 303, Gly 304, His 305, Ala 310, Ile 312, Thr 314, Trp 316, Asp 317, Arg 346, Phe 348, Gly 351, Asn 352, Asp 353, Val 354, Asp 356
3m	−7.32	4.31	TRP 59, TYR 62, GLN 63, VAL 98, HIS 101, LEU 162, LEU 165, ASP 197, ALA 198, SER 199, LYS 200, HIS 201, GLU 233, VAL 234, ILE 235
3n	−7.38	3.88	TRP 59, GLU 60, TYR 62, GLN 63, VAL 98, HIS 101, LEU 162, LEU 165, ASP 197, ALA 198, SER 199, LYS 200, HIS 201, GLU 233, VAL 234, ILE 235
3n	−7.1	6.29	TYR 67, LYS 68, LEU 69, CYS 70, ASN 75, GLU 76, ASP 77, CYS 115, VAL 129, LYS 178, GLU 181, TYR 182, HIS 185
3o	−7.67	2.40	ASP 451, ILE 453, SER 454, ILE 465, LYS 466, ILE 467, TYR 468, ALA 475, HIS 476, PHE 477, SER 478, ILE 479, SER 480, ALA 483, GLU 484, ASP 485, PHE 487, ILE 488
3o	−7.65	2.46	TRP 59, GLU 60, TYR 62, GLN 63, HIS 101, TYR 151, LEU 162, THR 163, LEU 165, ASP 197, ALA 198, SER 199, LYS 200, HIS 201, GLU 233, VAL 234, ILE 235
3o	−7.52	3.05	SER 66, TYR 67, LYS 68, LEU 69, CYS 70, ASN 75, GLU 76, ASP 77, CYS 115, ALA 128, VAL 129, LYS 178, GLU 181, TYR 182, HIS 185

M.p.: 213−215 °C; R_f: 0.44 (acetone/*n*-hexane, 1:3); λ_{max} = 283, 357 nm; FTIR (ATR) cm^{-1}: 3057 (=C−H stretching), 2937 (C−H aliphatic stretching), 1693 (C=N stretching), 1595 (thiazole skeletal vibrations), 1504, 1436 (C=C aromatic ring stretchings), 1305 (C−H aliphatic bending), 1093 (C−O stretching), 1024−731 (characteristic thiazole vibrations); ^{1}H NMR (400 MHz): δ (ppm) 8.29 (s, 1H, H−C=N−), 7.80 (dd, 2H, Ar−H, *J* = 9.0, 5.2 Hz), 7.49 (s, 1H, Ar−H), 7.19−7.13 (m, 2H, Ar−H), 7.03 (s, 1H, thiazole-H), 6.78 (s, 1H, Ar−H), 3.98 (s, 3H, $-OCH_3$), 3.94 (s, 3H, $-OCH_3$); ^{19}F NMR (375 MHz): δ (ppm) −114.53; ^{13}C NMR (100 MHz): δ (ppm) 168.7 (thiazole ring C2), 162.9(d, $^{1}J_{CF}$ = 248.3 Hz, Ar_{ipso}), 151.3 (Ar−C−O−Me), 148.8 (thiazole ring C4), 148.2, 142.7 (H−C=N−), 129.3, 127.7 (d, $^{3}J_{CF}$ = 8.4 Hz, Ar), 124.9, 115.9 (d, $^{2}J_{CF}$ = 21.6 Hz, Ar), 115.3 (d, $^{2}J_{CF}$ = 26.0 Hz, Ar), 108.7 (Ar−C), 102.5 (thiazole ring C5), 56.3 ($-OCH_3$), 56.0 ($-OCH_3$); HRMS: *m*/*z* calculated for $C_{18}H_{15}BrFN_3O_2S$, $[M + H]^+$: calcd: 436.0130, found: 436.0123; $[M + Na]^+$: calculated: 457.9950, found: 457.9934; $[2M + Na]^+$: calculated: 893.0002, found: 892.9978.

*2-(2-(2-Bromo-4-methylbenzylidene)hydrazinyl)-4-(4-fluorophenyl)thiazole (**3b**).* Light-yellow solid; yield: 80%; M.p.: 190−192 °C; R_f: 0.49 (acetone/*n*-hexane, 1:3); λ_{max} = 270, 357 nm; FTIR (ATR) cm^{-1}: 3192 (N−H stretching), 2974 (C−H aliphatic stretching), 1600 (C=N stretching), 1489 (thiazole skeletal vibrations), 1436 (C=C aromatic ring

https://doi.org/10.1021/acsomega.3c00265
ACS Omega 2023, 8, 11433−11446

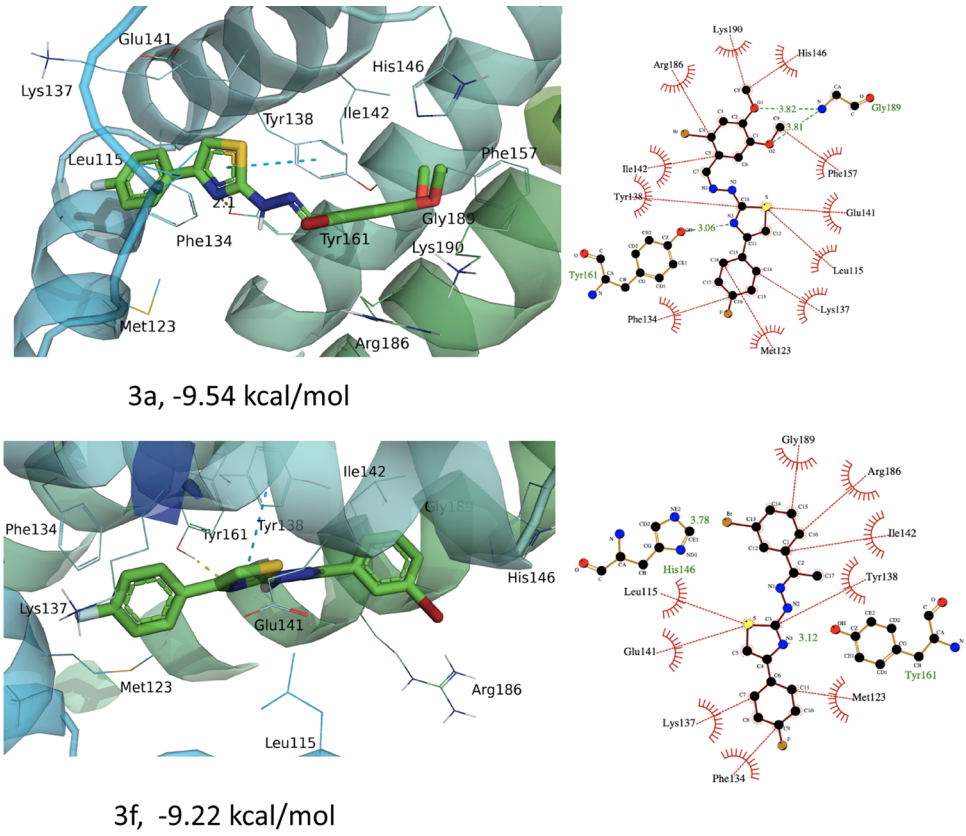

Figure 7. Best docking interactions are shown by ligands **3a** and **3f** with binding energies of −9.54 and −9.22 kj/mol against human serum albumin (HSA).

stretchings), 1039−837 (characteristic thiazole vibrations); ^{1}H NMR (400 MHz): δ (ppm) 12.35 (s, 1H, H−N−), 8.34 (s, 1H, H−C═N−), 7.89 (dd, 2H, Ar−H, J = 9.0, 5.6 Hz), 7.79 (d, 1H, Ar−H, J = 8.0 Hz), 7.50 (s, 1H, thiazole-H), 7.32 (s, 1H, Ar−H), 7.28−7.21 (m, 3H, Ar−H), 2.32 (s, 3H, $-CH_3$); ^{19}F NMR (375 MHz): δ (ppm) −114.57; ^{13}C NMR (100 MHz): δ (ppm) 168.5 (thiazole ring C2), 162.1 (d, $^{1}J_{CF}$ = 248.3 Hz, Ar_{ipso}), 150.0 (thiazole ring C4), 141.6 (H−C═N−), 140.0 (Ar−C−CH_3), 133.7, 131.7, 130.8, 129.4, 127.9 (d, $^{3}J_{CF}$ = 8.1 Hz, Ar−C), 126.7, 122.9, 115.9 (d, $^{2}J_{CF}$ = 21.6 Hz, Ar−C), 104.1 (thiazole ring C5), 20.9 ($-CH_3$); HRMS: m/z calculated for $C_{17}H_{13}BrFN_3S$, $[M + H]^+$: calcd: 390.0076, found: 390.0068; $[M + Na]^+$: calcd: 411.9896, found: 411.9885; $[2M + Na]^+$: calcd: 800.9894, found: 800.9878.

*4-(4-Fluorophenyl)-2-(2-(4-phenylbutan-2-ylidene)-hydrazinyl)thiazole (**3c**).* Beige solid; yield: 78%; M.p.: 181−183 °C; R_f: 0.53 (acetone/n-hexane, 1:3); λ_{max} = 278, 365 nm; FTIR (ATR) cm^{-1}: 3056 (═C−CH_3 stretching), 2951 (C−H aliphatic stretching), 1618 (C═N stretching), 1598 (thiazole skeletal vibrations), 1558, 1489 (C═C aromatic ring stretchings), 1448 (C−H aliphatic bending), 1037−700 (characteristic thiazole vibrations); ^{1}H NMR (400 MHz): δ (ppm) 7.75 (dd, 2H, Ar−H, J = 8.9, 5.1 Hz), 7.35−7.29 (m, 2H, Ar−H), 7.27−7.21 (m, 3H, Ar−H), 7.14 (t, 2H, Ar−H, J = 8.7 Hz), 6.73 (s, 1H, thiazole-H), 2.96 (t, 2H, $-CH_2-CH_2-$, J = 7.0 Hz), 2.70 (t, 2H, $-CH_2-CH_2-$, J = 7.0 Hz), 2.04 (s, 3H, $-CH_3$); ^{19}F NMR (375 MHz): δ (ppm) −114.63; ^{13}C NMR (100 MHz): δ (ppm) 169.7 (thiazole ring C2), 163.1 (d, $^{1}J_{CF}$ = 249.4 Hz, Ar_{ipso}), 155.7 (thiazole ring C4), 145.3(CH_3−C═N−), 140.9, 128.5 (d, $^{3}J_{CF}$ = 11.4 Hz, Ar−C), 127.7 (d, $^{3}J_{CF}$ = 8.1 Hz, Ar−C), 126.2, 116.1 (d, $^{2}J_{CF}$ = 21.6 Hz, Ar−C), 101.8 (thiazole ring C5), 40.0 ($-CH_2-CH_2-$C═N−), 32.2 ($-CH_2-CH_2-$), 17.2 (CH_3-CH_2-); HRMS: m/z calcd for $C_{19}H_{18}FN_3S$, $[M + H]^+$: calcd: 340.1283, found: 340.1273; $[M + Na]^+$: calculated: 362.1103, found: 362.1092; $[2M + Na]^+$: calcd: 701.2308, found: 701.2290.

*4-(4-Fluorophenyl)-2-(2-(4-(trifluoromethyl)benzylidene)-hydrazinyl)thiazole (**3d**).* Off-white solid; yield: 74%; M.p.: 166−168 °C; R_f: 0.44 (acetone/n-hexane, 1:3); λ_{max} = 268, 350 nm; FTIR (ATR) cm^{-1}: 1693 (C═N stretching), 1570 (thiazole skeletal vibrations), 1489, 1438 (C═C aromatic ring stretchings), 1409 (C−H aliphatic bending), 1035−729 (characteristic thiazole vibrations); ^{1}H NMR (400 MHz): δ (ppm) 8.26 (d, 1H, Ar−H, J = 8.3 Hz), 7.76 (ddt, 3H, Ar−H, J = 6.8, 5.4, 2.3 Hz), 7.69−7.63 (m, 3H, Ar−H), 7.16 (t, 2H, Ar−H, J = 8.7 Hz), 6.77 (s, 1H, thiazole-H); ^{19}F NMR (375 MHz): δ (ppm) −62.72, −112.97; ^{13}C NMR (100 MHz): δ (ppm) 170.6 (thiazole ring C2), 162.8 (d, $^{1}J_{CF}$ = 248.3 Hz, Ar_{ipso}), 148.9 (thiazole ring C4), 141.5, 137.3 (H−C═N−), 130.4, 128.1 (d, $^{2}J_{CF}$ = 8.1 Hz, Ar−C), 126.8 (Ar−C), 125.6 (d, $^{4}J_{CF}$ = 3.9 Hz, Ar−C), 115.9 (d, $^{2}J_{CF}$ = 21.6 Hz, Ar−C), 103.2 (thiazole ring C5); HRMS: m/z calculated for $C_{17}H_{11}F_4N_3S$, $[M + H]^+$: calcd: 366.0688, found: 366.0685; $[M + Na]^+$: calcd: 388.0508, found: 388.0508; $[2M + Na]^+$: calcd: 753.1118, found: 753.1098.

*4-(4-Fluorophenyl)-2-(2-((5-methylfuran-2-yl)methylene)-hydrazinyl)thiazole (**3e**).* Light-yellow solid; yield: 77%; M.p.: 142−143 °C; R_f: 0.50 (acetone/n-hexane, 1:3); λ_{max} = 278, 353 nm; FTIR (ATR) cm^{-1}: 2922 (C−H aliphatic stretching), 1610 (C═N stretching), 1490 (thiazole skeletal vibrations), 1450 (C═C aromatic ring stretchings), 1053−729 (characteristic thiazole vibrations); ^{1}H NMR (400 MHz): δ (ppm) 7.89

https://doi.org/10.1021/acsomega.3c00265
ACS Omega 2023, 8, 11433−11446

(d, 1H, furan-H, J = 5.5 Hz), 7.85 (s, 1H, H−C═N−), 7.30−7.18 (m, 3H, Ar−H), 7.13−7.03 (m, 1H, Ar−H), 6.69 (d, 1H, furan-H, J = 3.3 Hz), 6.22 (s, 1H, thiazol-H), 2.35 (s, 3H, CH_3−); ^{19}F NMR (375 MHz): δ (ppm) −114.63; ^{13}C NMR (100 MHz): δ (ppm) 168.5 (thiazole ring C2), 162.1 (d, $^1J_{CF}$ = 244.3 Hz, Ar_{ipso}), 154.4 (thiazole ring C4), 149.8 (furan C2), 148.3 (H−C═N− azomethine), 132.3 (furan C5), 130.4, 127.9 (d, $^3J_{CF}$ = 8.4 Hz, Ar−C), 115.9 (d, $^2J_{CF}$ = 21.6 Hz, Ar−C), 114.4 (furan C4), 108.9 (furan C3), 103.7 (thiazole ring C5), 14.0 (CH_3−); HRMS: m/z calcd for $C_{15}H_{12}FN_3OS$, $[M + H]^+$: 302.0763, found: 302.0749; $[M + Na]^+$: calcd: 324.0583, found: 324.0569; $[2M + Na]^+$: calcd: 625.1268, found: 625.1242.

*2-(2-(1-(3-Bromophenyl)ethylidene)hydrazinyl)-4-(4-fluorophenyl)thiazole (**3f**).* Orange solid; yield: 72%; M.p.: 120−122 °C; R_f: 0.52 (acetone/n-hexane, 1:3); λ_{max} = 267, 355 nm; FTIR (ATR) cm^{-1}: 1670 (C═N stretching), 1598 (thiazole skeletal vibrations), 1571, 1508, 1442 (C═C aromatic ring stretchings), 1029−696 (characteristic thiazole vibrations); ^{1}H NMR (400 MHz): δ (ppm) 11.39 (s, 1H, H−N−), 7.94 (s, 1H, Ar−H), 7.93−7.88 (m, 2H, Ar−H), 7.77 (d, 1H, Ar−H, J = 8.2 Hz), 7.57 (d, 1H, Ar−H, J = 8.9 Hz), 7.39 (t, 1H, Ar−H, J = 7.9 Hz), 7.32 (s, 1H, thiazole-H), 7.24 (t, 2H, Ar−H−C-F, J = 9.0 Hz), 2.32 (s, 3H, H_3C−C═N−); ^{19}F NMR (375 MHz): δ (ppm) −114.60; ^{13}C NMR (100 MHz): δ (ppm) 170.2 (thiazole ring C2), 162.1 (d, $^1J_{CF}$ = 244.3 Hz, Ar_{ipso}), 160.9 (thiazole ring C4), 145.3 (CH_3−C═N−), 140.8, 131.7, 131.1, 128.6,127.9 (d, $^3J_{CF}$ = 8.1 Hz, Ar−C), 125.2 (Ar−C), 122.4 (Ar−C−Br), 115.9 (d, $^2J_{CF}$ = 21.6 Hz, Ar−C), 104.5 (thiazole ring C5), 14.4 (CH_3−C═N−); HRMS: m/z calculated for $C_{17}H_{13}BrFN_3S$, $[M + H]^+$: calculated: 390.0076, found: 390.0071; $[M + Na]^+$: calculated: 411.9896, found: 411.9889; $[2M + Na]^+$: calculated: 800.9894, found: 800.9874.

*4-(4-Fluorophenyl)-2-(2-(1-(4-fluorophenyl)ethylidene)-hydrazinyl)thiazole (**3g**).* Lemon-yellow solid; yield: 70%; M.p.: 133−134 °C; R_f: 0.58 (acetone/n-hexane, 1:3); λ_{max} = 266, 350 nm; FTIR (ATR) cm^{-1}: 3057 (═C−H stretching), 2926 (C−H aliphatic stretching), 1605 (C═N stretching), 1485 (thiazole skeletal vibrations), 1442 (C═C aromatic ring stretchings), 1068−692 (characteristic thiazole vibrations); ^{1}H NMR (400 MHz): δ (ppm) 11.26 (s, 1H, H−N−), 7.92 (dd, 2H, Ar−H, J = 8.9, 5.5 Hz), 7.83 (dd, 2H, Ar−H, J = 9.0, 5.5 Hz), 7.31 (s, 1H, thiazole-H), 7.25 (td, 4H, Ar−H, J = 8.8, 6.3 Hz), 2.33 (s, 3H, −CH_3); ^{19}F NMR (375 MHz): δ (ppm) −113.23, −114.67; ^{13}C NMR (100 MHz): δ (ppm) 170.4 (thiazole ring C2), 163.7 (d, $^1J_{CF}$ = 244.3 Hz, Ar_{ipso}), 161.3 (d, $^1J_{CF}$ = 244.3 Hz, Ar_{ipso}), 150.1 (thiazole ring C4), 146.1 (H−C═N−), 134.9 (d, $^4J_{CF}$ = 3.3 Hz, Ar−C), 131.9 (Ar−C), 128.3 (d, $^3J_{CF}$ = 8.3 Hz, Ar−C), 127.9 (d, $^3J_{CF}$ = 8.3 Hz, Ar−C), 115.9 (d, $^3J_{CF}$ = 13.9 Hz, Ar−C−C−F), 115.7 (d, $^3J_{CF}$ = 13.9 Hz, Ar−C), 104.3 (thiazole ring C5), 14.5 (CH_3 −C═N−); HRMS: m/z calculated for $C_{17}H_{13}F_2N_3S$, $[M + H]^+$: calcd: 330.0876, found: 330.0865; $[M + Na]^+$: calcd: 352.0696, found: 352.0682; $[2M + Na]^+$: calcd: 681.1494, found: 681.1464.

*4-Chloro-2-((2-(4-(4-fluorophenyl)thiazol-2-yl)-hydrazinylidene)methyl)phenol (**3h**).* Orange solid; yield: 66%; M.p.: 192−193 °C; R_f: 0.27 (acetone/n-hexane, 1:3); λ_{max} = 265, 358 nm; FTIR (ATR) cm^{-1}: 3138 (O−H stretching), 3101 (═C−H stretching), 2924 (C−H aliphatic stretching), 1610 (C═N stretching), 1562 (thiazole skeletal vibrations), 1477 (C═C aromatic ring stretchings), 1031−734 (characteristic thiazole vibrations); ^{1}H NMR (400 MHz): δ (ppm) 12.25 (s, 1H, H−N−), 10.36 (s, 1H, H−O), 8.28 (s, 1H, H−C═N−), 7.89 (dd, 2H, Ar−H, J = 8.8, 5.6 Hz), 7.63 (d, 2H, Ar−H, J = 2.8 Hz), 7.30 (s, 1H, thiazole-H), 7.28−7.17 (m, 3H, Ar−H), 6.93 (d, 1H, Ar−H, J = 8.8 Hz); ^{19}F NMR (375 MHz): δ (ppm) −114.49; ^{13}C NMR (100 MHz): δ (ppm) 168.5 (thiazole ring C2), 162.1 (d, $^1J_{CF}$ = 244.7 Hz, Ar_{ipso}), 155.1 (thiazole ring C4), 149.1(Ar−C−OH), 137.8 (H−C═N−), 131.7, 130.3 (Ar−C), 127.9 (d, $^3J_{CF}$ = 8.1 Hz, Ar−C), 125.2 (Ar−C), 123.7 (Ar−C-Cl), 122.6, 118.4 (Ar−C), 115.9 (d, $^3J_{CF}$ = 21.3 Hz, Ar−C), 103.8 (thiazole ring C5); HRMS: m/z calcd for $C_{16}H_{11}ClFN_3OS$, $[M + H]^+$: calcd: 348.0373, found: 348.0365; $[M + Na]^+$: calcd: 370.0193, found: 370.0190; $[2M + Na]^+$: calcd: 717.0488, found: 717.0472.

*4-(4-Fluorophenyl)-2-(2-(3-(trifluoromethyl)benzylidene)-hydrazinyl)thiazole (**3i**).* Gray solid; yield: 72%; M.p.: 157−159 °C; R_f: 0.38 (acetone/n-hexane, 1:3); λ_{max} = 264, 358 nm; FTIR (ATR) cm^{-1}: 3061 (═C−H stretching), 2929 (C−H aliphatic stretching), 1695 (C═N stretching), 1570 (thiazole skeletal vibrations), 1500, 1448 (C═C aromatic ring stretchings), 1068−736 (characteristic thiazole vibrations); ^{1}H NMR (400 MHz): δ (ppm) 8.13 (s, 1H, H−C═N−), 7.97 (d, 2H, Ar−H, J = 8.7 Hz), 7.90 (dd, Ar−H, J = 8.9, 5.5 Hz), 7.73−7.65 (m, 2H, Ar−H), 7.34 (s, 1H, thiazole-H), 7.24 (t, 2H, Ar−H, J = 8.8 Hz); ^{19}F NMR (375 MHz): δ (ppm) −61.39, −114.54; ^{13}C NMR (100 MHz): δ (ppm) 168.6 (thiazole ring C2), 162.1 (d, $^1J_{CF}$ = 244.7 Hz, Ar_{ipso}), 150.0 (thiazole ring C4), 139.9 (H−C═N−), 136.1, 131.7 (d, $^4J_{CF}$ = 3.3 Hz, Ar−C), 130.4 (d, $^3J_{CF}$ = 11.7 Hz, Ar−C), 129.9, 127.9 (d, $^3J_{CF}$= 8.1 Hz, Ar−C), 125.9, 123.2, 122.9 (d, $^4J_{CF}$ = 4.0 Hz, Ar−C), 115.9 (d, $^2J_{CF}$ = 21.3 Hz, Ar−C), 104.3 (thiazole ring C5); HRMS: m/z calcd for $C_{17}H_{11}F_4N_3S$, $[M + H]^+$: calcd: 366.0688, found: 366.0680; $[2M + Na]^+$: calcd: 753.1118, found: 753.1086.

*2-(2-(2-Ethoxybenzylidene)hydrazinyl)-4-(4-fluorophenyl)thiazole (**3j**).* Light-yellow solid; yield: 78%; M.p.: 127−128 °C; R_f: 0.40 (acetone/n-hexane, 1:3); λ_{max} = 265, 370 nm; FTIR (ATR) cm^{-1}: 2930 (C−H aliphatic stretching), 1607 (C═N stretching), 1500 (thiazole skeletal vibrations), 1495, 1457 (C═C aromatic ring stretchings), 1018−703 (characteristic thiazole vibrations); ^{1}H NMR (400 MHz): δ (ppm) 8.41 (s, 1H, H−C═N−), 7.89 (dd, Ar−H, J = 8.9, 5.5 Hz), 7.79 (d, 1H, Ar−H, J = 7.8 Hz), 7.37−7.20 (m, 4H, Ar−H), 7.08−6.95 (m, 3H, Ar−H), 4.14−4.07 (m, 2H, −CH_2−CH_3), 1.38 (t, 3H, CH_3−CH_2−, J = 7.0 Hz); ^{19}F NMR (375 MHz): δ (ppm) −114.63; ^{13}C NMR (100 MHz): δ (ppm) 168.8 (thiazole ring C2), 164.7 (d, $^1J_{CF}$ = 285.4 Hz, Ar_{ipso}), 160.9 (Ar−C−O) 156.9, 149.9 (thiazole ring C4), 137.7 (H−C═N−), 131.8 (d, $^4J_{CF}$ = 2.9 Hz, Ar−C), 131.1 (Ar−C), 127.9 (d, J = 8.1 Hz, Ar−C), 125.4, 123.1, 121.2 (Ar−C), 115.9 (d, $^2J_{CF}$ = 21.3 Hz), 113.3 (Ar−C), 103.8 (thiazole ring C5), 64.3 (CH_3−CH_2−O−), 15.1 (CH_3−CH_2−); HRMS: m/z calculated for $C_{18}H_{16}FN_3OS$, $[M + H]^+$: calcd: 342.1076, found: 342.1058; $[M + Na]^+$: calcd: 364.0896, found: 364.0882; $[2M + Na]^+$: calcd: 705.1894, found: 705.1853.

*4-(4-Fluorophenyl)-2-(2-(2-(trifluoromethyl)benzylidene)-hydrazinyl)thiazole (**3k**).* Off-white solid; yield: 79%; M.p.: 168−169 °C; R_f: 0.49 (acetone/n-hexane, 1:3); λ_{max} = 265, 364 nm; FTIR (ATR) cm^{-1}: 3057 (═C−H stretching), 2933 (C−H aliphatic stretching), 1699 (C═N stretching), 1572 (thiazole skeletal vibrations), 1499, 1446 (C═C aromatic ring stretchings), 1060−734 (characteristic thiazole vibrations); ^{1}H

https://doi.org/10.1021/acsomega.3c00265
ACS Omega 2023, 8, 11433−11446

NMR (400 MHz): δ (ppm) 12.50 (s, 1H, H−N−), 8.37 (s, 1H, H−C═N−), 8.14 (d, 1H, Ar−H, J = 7.8 Hz), 7.90 (dd, 2H, Ar−H, J = 8.8, 5.6 Hz), 7.81−7.72 (m, 2H, Ar−H), 7.58 (t, 1H, Ar−H, J = 7.6 Hz), 7.37 (s, 1H, thiazole-H), 7.25 (t, 2H, Ar−H, J = 8.9 Hz); ^{19}F NMR (375 MHz): δ (ppm) −57.06, −114.48; ^{13}C NMR (100 MHz): δ (ppm) 168.3 (thiazole ring C2), 162.1 (d, $^{1}J_{CF}$ = 244.7 Hz, Ar_{ipso}), 150.1 (thiazole ring C4), 136.6 (H−C═N−), 133.3, 132.7, 131.6, 129.7, 128.1 (d, $^{3}J_{CF}$ = 8.1 Hz, Ar−C), 127.9, 126.6−126.1 (m, Ar−C), 115.9 (d, $^{2}J_{CF}$ = 21.6 Hz, Ar−C), 104.5 (thiazole ring C5); HRMS: m/z calculated for $C_{17}H_{11}F_4N_3S$, $[M + H]^+$: calcd: 366.0688, found: 366.0680; $[2M + Na]^+$: calcd: 753.1118, found: 753.1086.

*2-(2-(3-Fluoro-2-methoxybenzylidene)hydrazinyl)-4-(4-fluorophenyl)thiazole (**3l**).* Light-yellow solid; yield: 61%; M.p.: 115−117 °C; R_f: 0.39 (acetone/n-hexane, 1:3); λ_{max} = 276, 368 nm; FTIR (ATR) cm^{-1}: 3055 (═C−H stretching), 1604 (C═N stretching), 1575 (thiazole skeletal vibrations), 1489, 1444 (C═C aromatic ring stretching), 1006−696 (characteristic thiazole vibrations); ^{1}H NMR (400 MHz): δ (ppm) 8.29 (s, 1H, H−C═N−), 7.90 (dd, 2H, Ar−H, J = 8.9, 5.5 Hz), 7.63 (d, 1H, Ar−H, J = 8.0 Hz), 7.33 (s, 1H, thiazole-H), 7.31−7.21 (m, 3H, Ar−H), 7.18 (td, 1H, Ar−H, J = 8.2, 5.1 Hz), 3.91 (s, 3H, $-CH_3$); ^{19}F NMR (375 MHz): δ (ppm) −114.55, −131.04; ^{13}C NMR (100 MHz): δ (ppm) 168.6 (thiazole ring C2), 162.1 (d, $^{1}J_{CF}$ = 244.3 Hz, Ar_{ipso}), 155.7 (d, $^{1}J_{CF}$ = 245.0 Hz, Ar_{ipso}), 150.0 (thiazole C4), 145.8 (Ar−C−O), 136.1 (H−C═N−), 131.7 (d, $^{4}J_{CF}$ = 2.9 Hz, Ar−C), 129.5 (d, $^{4}J_{CF}$ = 2.9 Hz, Ar−C), 127.9 (d, $^{3}J_{CF}$ = 8.4 Hz, Ar−C), 124.9 (d, $^{3}J_{CF}$ = 8.1 Hz, Ar−C), 121.1 (d, $^{4}J_{CF}$ = 3.3 Hz, Ar−C), 117.8 (d, $^{2}J_{CF}$ = 19.1 Hz, Ar−C), 115.9 (d, $^{2}J_{CF}$ = 21.6 Hz, Ar−C), 104.2 (thiazole ring C5), 62.5 (d, $^{5}J_{HF}$ = 5.1 Hz, $-OCH_3$); HRMS: m/z calculated for $C_{17}H_{13}F_2N_3OS$, $[M + H]^+$: calcd: 346.0825, found: 346.0823; $[M + Na]^+$: calcd: 368.0645, found: 368.0642; $[2M + Na]^+$: calcd: 713.1392, found: 713.1378.

*2-(2-((1H-Pyrrol-2-yl)methylene)hydrazinyl)-4-(4-fluorophenyl)thiazole (**3m**).* Dark-gray solid; yield: 77%; M.p.: 130−132 °C; R_f: 0.45 (acetone/n-hexane, 1:3); λ_{max} = 282, 358 nm; FTIR (ATR) cm^{-1}: 3278 (N−H stretching), 1626 (C═N stretching), 1593 (thiazole skeletal vibrations), 1500 (C═C aromatic ring stretchings), 1029−730 (characteristic thiazole vibrations); ^{1}H NMR (400 MHz): δ (ppm) 11.77 (s, 1H, H−N−), 11.21 (s, 1H, H−N, pyrrole), 7.91 (s, 1H, H−C═N−), 7.88 (dd, 2H, Ar−H, J = 8.9, 5.6 Hz), 7.30−7.18 (m, 3H, Ar−H), 6.90 (d, 1H, pyrrole-H, J = 1.5 Hz), 6.40 (s, 1H, thiazole), 6.12 (d, 1H, pyrrole-H, J = 3.6 Hz); ^{19}F NMR (375 MHz): δ (ppm) −114.77; ^{13}C NMR (100 MHz): δ (ppm) 168.8 (thiazole ring C2), 162.0 (d, $^{1}J_{CF}$ = 244.3 Hz, Ar_{ipso}), 154.7 (thiazole ring C4), 149.7, 135.5 (H−C═N−), 131.9 (pyrrole C2), 127.9 (d, $^{3}J_{CF}$ = 8.1 Hz, Ar−C), 127.6 (Ar−C), 122.1 (pyrrole C3), 115.9 d, $^{2}J_{CF}$ = 21.6 Hz, 111.8 (Ar−C), 109.6 (pyrrole-C5), 103.3 (thiazole ring C5).

*4-(4-Fluorophenyl)-2-(2-(thiophen-2-ylmethylene)-hydrazinyl)thiazole (**3n**).* Yellow solid; yield: 67%; M.p.: 143−145 °C; R_f: 0.54 (acetone/n-hexane, 1:3); λ_{max} = 279, 358 nm; FTIR (ATR) cm^{-1}: 1602 (C═N stretching), 1479 (C═C aromatic ring stretching), 1004−777 (characteristic thiazole vibrations); ^{1}H NMR (400 MHz): δ (ppm) 8.23 (s, 1H, H−C═N−), 7.89 (dd, 2H, Ar−C, J = 8.9, 5.6 Hz), 7.58 (d, 1H, thiophene C5−H, J = 5.0 Hz), 7.37 (d, 1H, thiophene C3−H, J = 2.5 Hz), 7.29 (s, 1H, thiazole-H), 7.24 (t, 2H, Ar−H, J = 8.9 Hz), 7.10 (dd, 1H, Ar−H, J = 5.1, 3.5 Hz); ^{19}F NMR (375 MHz): δ (ppm) −114.57; ^{13}C NMR (100 MHz): δ (ppm) 168.4 (thiazole ring C2), 162.1 (d, $^{1}J_{CF}$ = 244.3 Hz, Ar_{ipso}), 149.9 (thiophene C2), 139.6 (thiophene C3), 137.2 (H−C═N−), 131.7, 129.6, 128.2 (d, $^{2}J_{CF}$ = 18.0 Hz, Ar−C), 127.9 (d, $^{3}J_{CF}$ = 8.1 Hz, Ar−C), 115.9 (d, $^{2}J_{CF}$ = 21.3 Hz, Ar−C), 103.9 (thiazole ring C5); HRMS: m/z calcd for $C_{14}H_{10}FN_3S_2$, $[M + H]^+$: calcd: 304.0378, found: 304.0375; $[M + Na]^+$: calcd: 326.0198, found: 326.0193; $[2M + Na]^+$: calcd: 629.0498, found: 629.0487.

*4-(4-Fluorophenyl)-2-(2-(2-(methylthio)benzylidene)-hydrazinyl)thiazole (**3o**).* Pink solid; yield: 80%; M.p.: 152−154 °C; R_f: 0.48 (acetone/n-hexane, 1:3); λ_{max} = 287, 357 nm; FTIR (ATR) cm^{-1} = 3138 (N−H stretching), 3053 (═C−H stretching), 1601 (C═N stretching), 1489, 1446 (C═C aromatic ring stretchings), 1411 (C−H aliphatic bending), 1006−731 (characteristic thiazole vibrations); ^{1}H NMR (400 MHz): δ (ppm) 8.43 (s, 1H, H−C═N−), 7.90 (dd, 2H, Ar−C, J = 8.9, 5.5 Hz), 7.74 (d, 1H, Ar−H, J = 8.5 Hz), 7.40−7.33 (m, 2H, Ar−H), 7.31 (s, 1H, thiazole-H), 7.24 (td, 3H, Ar−H, J = 8.5, 3.7 Hz), 2.50 (s, 3H, CH_3−S); ^{19}F NMR (375 MHz): δ (ppm) −114.53; ^{13}C NMR (100 MHz): δ (ppm) 168.7 (thiazole ring C2), 162.1 (d, $^{1}J_{CF}$ = 244.3 Hz, Ar_{ipso}), 149.9 (thiazole C4), 139.6 (H−C═N−), 137.8 (Ar−C−S), 132.2, 131.7 (d, $^{4}J_{CF}$ = 3.3 Hz, Ar−C), 130.0, 127.9 (d, $^{3}J_{CF}$ = 8.1 Hz, Ar−C), 127.0 (d, $^{2}J_{CF}$ = 30.1 Hz, Ar−C), 125.7, 115.9 (d, $^{2}J_{CF}$ = 21.6 Hz, Ar−C), 104.1 (thiazole ring C5), 16.2 (CH_3−S); HRMS: m/z calculated for $C_{17}H_{14}FN_3S_2$; $[M + H]^+$: calcd: 344.0691, found: 344.0688; $[M + Na]^+$: calcd: 366.0511, found: 366.0507; $[2M + Na]^+$: calcd: 709.1124, found: 709.1124.

(Please see the Supporting Information for protocols of α-amylase, antiglycation inhibition, antioxidant, *in vitro* hemolysis, and molecular docking studies).

■ ASSOCIATED CONTENT

Supporting Information

The Supporting Information is available free of charge at https://pubs.acs.org/doi/10.1021/acsomega.3c00265.

UV−vis, FTIR, ^{1}H, ^{13}C, ^{19}F NMR, and HRMS spectra of all compounds, and protocols of all biological assays along with molecular docking experiment (PDF)

■ AUTHOR INFORMATION

Corresponding Authors

Muhammad Khalid − *Institute of Chemistry, Khwaja Fareed University of Engineering & Information Technology, Rahim Yar Khan 64200, Pakistan; Center for Theoretical and Computational Research, Khwaja Fareed University of Engineering & Information Technology, Rahim Yar Khan 64200, Pakistan;* orcid.org/0000-0002-1899-5689; Email: muhammad.khalid@kfueit.edu.pk, Khalid@iq.usp.br

Tashfeen Akhtar − *Department of Chemistry, Mirpur University of Science and Technology (MUST), Mirpur 10250 Azad Jammu and Kashmir, Pakistan*; Email: tashfeenchem@must.edu.pk

Raha Orfali − *Department of Pharmacognosy, Collage of Pharmacy, King Saud University, Riyadh 11451, Saudi Arabia*; Email: rorfali@ksu.edu.sa

https://doi.org/10.1021/acsomega.3c00265
ACS Omega 2023, 8, 11433−11446

Authors

Hasnain Mehmood − *Department of Chemistry, Mirpur University of Science and Technology (MUST), Mirpur 10250 Azad Jammu and Kashmir, Pakistan*

Muhammad Haroon − *Department of Chemistry, Mirpur University of Science and Technology (MUST), Mirpur 10250 Azad Jammu and Kashmir, Pakistan; Department of Chemistry, Government Major Muhammad Afzal Khan (Shaheed), Boys Degree College Afzalpur, Mirpur (Affiliated with Mirpur University of Science and Technology (MUST)), Mirpur 10250 Azad Jammu and Kashmir, Pakistan*

Simon Woodward − *GSK, Carbon Neutral Laboratories for Sustainable Chemistry, University Park Nottingham, Nottingham NG7 2RD, U.K.;* orcid.org/0000-0001-8539-6232

Muhammad Adnan Asghar − *Department of Chemistry, Division of Science and Technology, University of Education, Lahore 54770, Pakistan*

Rabia Baby − *Department of Education, Sukkur IBA University, Sukkur 65200 Sindh, Pakistan*

Shagufta Perveen − *Department of Chemistry, School of Computer, Mathematical and Natural Sciences, Morgan State University, Baltimore, Maryland 21251, United States*

Complete contact information is available at: https://pubs.acs.org/10.1021/acsomega.3c00265

Author Contributions

Dr. Muhammad Khalid, confirm that all authors played their role in this work and is briefed as follows: H.M.: performed all experimental work, characterization, and write-up; M.H.: data compilation, assisting in syntheses, and write-up; T.A.: supervisor of the first author, designed the project, refined the paper, and also corresponding author; S.W.: assisted first author (characterization) in his lab, paper writing, and improvement; M.K., M.A.A., R.B., R.O., S.P.: molecular docking and writing of the part.

Notes

The authors declare no competing financial interest.

■ ACKNOWLEDGMENTS

The authors extend their appreciation to the Researcher Supporting Project number (RSP2023R431), King Saud University, Riyadh, Saudi Arabia, for funding this research work. Dr. Muhammad Khalid gratefully acknowledges the financial support of HEC Pakistan (project no. 20-14703/NRPU/R&D/HEC/2021). H.M. is thankful to HEC Pakistan for the award of IRSIP fellowship for the University of Nottingham. The authors are also thankful for the cooperation and collaboration of A.A.C.B from IQ-USP, Brazil, especially for his continuous support and providing computational lab facilities.

■ REFERENCES

(1) Carroll, A. R.; Copp, B. R.; Davis, R. A.; Keyzers, R. A.; Prinsep, M. R. Marine natural products. *Nat. Prod. Rep.* **2021**, *38*, 362−413.

(2) Álvarez-Martínez, F. J.; Barrajón-Catalán, E.; Micol, V. Tackling antibiotic resistance with compounds of natural origin: A comprehensive review. *Biomedicines* **2020**, *8*, No. 405.

(3) Cabrita, M. T.; Vale, C.; Rauter, A. P. Halogenated compounds from marine algae. *Mar. Drugs* **2010**, *8*, 2301−2317.

(4) Neumann, C. S.; Fujimori, D. G.; Walsh, C. T. Halogenation strategies in natural product biosynthesis. *Chem. Biol.* **2008**, *15*, 99−109.

(5) Ebied, A. M.; Elmariah, H.; Cooper-DeHoff, R. M. New Drugs Approved in 2021. *Am. J. Med.* **2022**, *135*, 836−839.

(6) FDA, U. New drugs at FDA: CDER's new molecular entities and new therapeutic biological products 2020.

(7) Burant, C. F.; Treutelaar, M. K.; Peavy, D. E.; Frank, B. H.; Buse, M. G. Differential binding of monoidinated insulins to muscle and liver derived receptors and activation of the receptor kinase. *Biochem. Biophys. Res. Commun.* **1988**, *152*, 1353−1360.

(8) Dumas, J. Cx4... Base Interaction as Models of Weak Charge-Transfer Interactions: Comparison With Strong ChargeTransfer and Hydrogen-Bond Interactions 1978.

(9) Voth, A. R.; Hays, F. A.; Ho, P. S. Directing macromolecular conformation through halogen bonds. *Proc. Natl. Acad. Sci. U.S.A.* **2007**, *104*, 6188−6193.

(10) Metrangolo, P.; Meyer, F.; Pilati, T.; Resnati, G.; Terraneo, G. Halogen bonding in supramolecular chemistry. *Angew. Chem., Int. Ed.* **2008**, *47*, 6114−6127.

(11) Cody, V.; Murray-Rust, P. Iodine··· X (O, N, S) intermolecular contacts: models of thyroid hormone— protein binding interactions using information from the cambridge crystallographic data files. *J. Mol. Struct.* **1984**, *112*, 189−199.

(12) Wilcken, R.; Zimmermann, M. O.; Lange, A.; Joerger, A. C.; Boeckler, F. M. Principles and applications of halogen bonding in medicinal chemistry and chemical biology. *J. Med. Chem.* **2013**, *56*, 1363−1388.

(13) Metrangolo, P.; Resnati, G. *Halogen Bonding: Fundamentals and Applications*; Springer, 2008; Vol. *126*.

(14) Tiz, D. B.; Bagnoli, L.; Rosati, O.; Marini, F.; Sancineto, L.; Santi, C. New Halogen-Containing Drugs Approved by FDA in 2021: An Overview on Their Syntheses and Pharmaceutical Use. *Molecules* **2022**, *27*, No. 1643.

(15) Eskandari, K.; Lesani, M. Does fluorine participate in halogen bonding? *Chem. - Eur. J.* **2015**, *21*, 4739−4746.

(16) Inoue, M.; Sumii, Y.; Shibata, N. Contribution of organo-fluorine compounds to pharmaceuticals. *ACS Omega* **2020**, *5*, 10633−10640.

(17) Morgenthaler, M.; Schweizer, E.; Hoffmann-Röder, A.; Benini, F.; Martin, R. E.; Jaeschke, G.; Wagner, B.; Fischer, H.; Bendels, S.; Zimmerli, D.; et al. Predicting and tuning physicochemical properties in lead optimization: amine basicities. *ChemMedChem* **2007**, *2*, 1100−1115.

(18) Shah, P.; Westwell, A. D. The role of fluorine in medicinal chemistry. *J. Enzyme Inhib. Med. Chem.* **2007**, *22*, 527−540.

(19) Mei, H.; Han, J.; Fustero, S.; Medio-Simon, M.; Sedgwick, D. M.; Santi, C.; Ruzziconi, R.; Soloshonok, V. A. Fluorine-containing drugs approved by the FDA in 2018. *Chem. - Eur. J.* **2019**, *25*, 11797−11819.

(20) Muller, K.; Faeh, C.; Diederich, F. Fluorine in pharmaceuticals: looking beyond intuition. *Science* **2007**, *317*, 1881−1886.

(21) Yu, Y.; Liu, A.; Dhawan, G.; Mei, H.; Zhang, W.; Izawa, K.; Soloshonok, V. A.; Han, J. Fluorine-containing pharmaceuticals approved by the FDA in 2020: Synthesis and biological activity. *Chin. Chem. Lett.* **2021**, *32*, 3342−3354.

(22) Ali, M.; Khan, K. M.; Salar, U.; Ashraf, M.; Taha, M.; Wadood, A.; Hamid, S.; Riaz, M.; Ali, B.; Shamim, S. Synthesis, in vitro-glucosidase inhibitory activity, and in silico study of (E)-thiosemicarbazones and (E)-2-(2-(arylmethylene) hydrazinyl)-4-arylthiazole derivatives 2018.

(23) Salar, U.; Khan, K. M.; Syed, S.; Taha, M.; Ali, F.; Ismail, N. H.; Perveen, S.; Wadood, A.; Ghufran, M. Synthesis, in vitro β-glucuronidase inhibitory activity and in silico studies of novel (E)-4-Aryl-2-(2-(pyren-1-ylmethylene) hydrazinyl) thiazoles. *Bioorg. Chem.* **2017**, *70*, 199−209.

(24) de Oliveira Filho, G. B.; de Oliveira Cardoso, M. V.; Espíndola, J. W. P.; e Silva, D. A. O.; Ferreira, R. S.; Coelho, P. L.; Dos Anjos, P. S.; de Souza Santos, E.; Meira, C. S.; Moreira, D. R. M.; et al. Structural design, synthesis and pharmacological evaluation of thiazoles against Trypanosoma cruzi. *Eur. J. Med. Chem.* **2017**, *141*, 346−361.

(25) Costa, L. B.; de Oliveira Cardoso, M. V.; de Oliveira Filho, G. B.; de Moraes Gomes, P. A. T.; Espíndola, J. W. P.; de Jesus Silva, T. G.; Torres, P. H. M.; Silva, F. P.; Silva, F. P., Jr.; Martin, J.; de Figueiredo, R. C. B. Q.; Leite, A. C. L. Compound profiling and 3D-QSAR studies of hydrazone derivatives with activity against intracellular Trypanosoma cruzi. *Bioorg. Med. Chem.* **2016**, *24*, 1608−1618.
(26) Khan, K. M.; Irfan, M.; Ashraf, M.; Taha, M.; Saad, S. M.; Perveen, S.; Choudhary, M. I. Synthesis of phenyl thiazole hydrazones and their activity against glycation of proteins. *Med. Chem. Res.* **2015**, *24*, 3077−3085.
(27) Salar, U.; Khan, K. M.; Chigurupati, S.; Taha, M.; Wadood, A.; Vijayabalan, S.; Ghufran, M.; Perveen, S. New hybrid hydrazinyl thiazole substituted chromones: As potential α-amylase inhibitors and radical (DPPH & ABTS) scavengers. *Sci. Rep.* **2017**, *7*, No. 16980.
(28) Pathania, S.; Narang, R. K.; Rawal, R. K. Role of sulphur-heterocycles in medicinal chemistry: An update. *Eur. J. Med. Chem.* **2019**, *180*, 486−508.
(29) Shahzadi, K.; Haroon, M.; Khalid, M.; Akhtar, T.; Ghous, T.; Alam, M. M.; Imran, M. Synthesis and in Silico Docking Studies of Ethyl 2-(2-Arylidene-1-alkylhydrazinyl) thiazole-4-carboxylates as Antiglycating Agents. *Chem. Biodiversity* **2022**, *19*, No. e202100581.
(30) Mehmood, H.; Haroon, M.; Akhtar, T.; Woodward, S.; Andleeb, H. Synthesis and molecular docking studies of 5-acetyl-2-(arylidenehydrazin-1-yl)-4-methyl-1, 3-thiazoles as α-amylase inhibitors. *J. Mol. Struct.* **2022**, *1250*, No. 131807.
(31) Mehmood, H.; Akhtar, T.; Haroon, M.; Tahir, E.; Ehsan, M.; Woodward, S.; Musa, M. Synthesis of Arylidenehydrazinyl-4-methoxyphenylthiazole Derivatives: Docking Studies, Probing Type II Diabetes Complication Management Agents. *Chem. Biodiversity* **2022**, *19*, No. e202200824.
(32) Khan, K. M.; Shah, Z.; Ahmad, V. U.; Khan, M.; Taha, M.; Rahim, F.; Jahan, H.; Perveen, S.; Choudhary, M. I. Synthesis of 2, 4, 6-trichlorophenyl hydrazones and their inhibitory potential against glycation of protein. *Med. Chem.* **2011**, *7*, 572−580.
(33) Taha, M.; Naz, H.; Rasheed, S.; Ismail, N. H.; Rahman, A. A.; Yousuf, S.; Choudhary, M. I. Synthesis of 4-methoxybenzoylhydrazones and evaluation of their antiglycation activity. *Molecules* **2014**, *19*, 1286−1301.
(34) Taha, M.; Noreen, T.; Imran, S.; Nawaz, F.; Chigurupati, S.; Selvaraj, M.; Rahim, F.; Ismail, N. H.; Kumar, A.; Mosaddik, A.; et al. Synthesis, α-amylase inhibition and molecular docking study of bisindolylmethane sulfonamide derivatives. *Med. Chem. Res.* **2019**, *28*, 2010−2022.
(35) Taha, M.; Alkadi, K. A.; Ismail, N. H.; Imran, S.; Adam, A.; Kashif, S. M.; Shah, S. A. A.; Jamil, W.; Sidiqqui, S.; Khan, K. M. Antiglycation and antioxidant potential of novel imidazo [4, 5-b] pyridine benzohydrazones. *Ar. J. Chem.* **2019**, *12*, 3118−3128.
(36) Ullah, S.; Mirza, S.; Salar, U.; Hussain, S.; Javaid, K.; Khan, K. M.; Khalil, R.; Atia-tul-Wahab; Ul-Haq, Z.; Perveen, S.; Choudhary, M. I. 2-Mercapto Benzothiazole Derivatives: As Potential Leads for the Diabetic Management. *Med. Chem.* **2020**, *16*, 826−840.
(37) Taurins, A.; Fenyes, J.; Jones, R. N. Thiazoles: iii. Infrared spectra of methylthiazoles. *Can. J. Chem.* **1957**, *35*, 423−427.
(38) Malik, A.; Mehmood, M. H.; Fayyaz-ur-Rehman, M. Journey of 100 Years of Insulin Discovery, From Past to Present: An Overview. *Multidiscip. Rev.* **2021**, *1*, 19−34.
(39) Di Muzio, E.; Polticelli, F.; Trezza, V.; Fanali, G.; Fasano, M.; Ascenzi, P. Imatinib binding to human serum albumin modulates heme association and reactivity. *Arch. Biochem. Biophys.* **2014**, *560*, 100−112.
(40) Shahzadi, K.; Haroon, M.; Khalid, M.; Akhtar, T.; Ghous, T.; Alam, M. M.; Imran, M. Synthesis and in Silico Docking Studies of Ethyl 2-(2-Arylidene-1-alkylhydrazinyl)thiazole-4-carboxylates as Antiglycating Agents. *Chem. Biodiversity* **2022**, *19*, No. e202100581.
(41) Ascenzi, P.; di Masi, A.; Fanali, G.; Fasano, M. Heme-based catalytic properties of human serum albumin. *Cell Death Discovery* **2015**, *1*, No. 15025.
(42) Purnamasari, V.; Estiasih, T.; Sujuti, H.; Widjanarko, S. B. Identification of phenolic acids of Pandan anggur (Sararanga sinuosa Hemsley) fruits and their potential antiglycation through molecular docking study. *J. Appl. Pharm. Sci.* **2021**, *11*, 126−134.
(43) Fanali, G.; Di Masi, A.; Trezza, V.; Marino, M.; Fasano, M.; Ascenzi, P. Human serum albumin: from bench to bedside. *Mol. Aspects Med.* **2012**, *33*, 209−290.
(44) Rondeau, P.; Bourdon, E. The glycation of albumin: structural and functional impacts. *Biochimie* **2011**, *93*, 645−658.
(45) Rabbani, G.; Ahn, S. N. Structure, enzymatic activities, glycation and therapeutic potential of human serum albumin: A natural cargo. *Int. J. Biol. Macromol.* **2019**, *123*, 979−990.
(46) Shaikh, M.; Siddiqui, S.; Zafar, H.; Naqeeb, U.; Subzwari, F.; Imad, R.; Khan, K. M.; Choudhary, M. I. Antiglycation Activity of Triazole Schiff's Bases Against Fructosemediated Glycation: In Vitro and In Silico Study. *Med. Chem.* **2020**, *16*, 575−591.
(47) Brayer, G. D.; Luo, Y.; Withers, S. G. The structure of human pancreatic alpha-amylase at 1.8 A resolution and comparisons with related enzymes. *Protein Sci.* **1995**, *4*, 1730−1742.
(48) Dandekar, P. D.; Kotmale, A. S.; Chavan, S. R.; Kadlag, P. P.; Sawant, S. V.; Dhavale, D. D.; RaviKumar, A. Insights into the Inhibition Mechanism of Human Pancreatic α-Amylase, a Type 2 Diabetes Target, by Dehydrodieugenol B Isolated from Ocimum tenuiflorum. *ACS Omega* **2021**, *6*, 1780−1786.
(49) Akinyede, K. A.; Oyewusi, H. A.; Hughes, G. D.; Ekpo, O. E.; Oguntibeju, O. O. In Vitro Evaluation of the Anti-Diabetic Potential of Aqueous Acetone Helichrysum petiolare Extract (AAHPE) with Molecular Docking Relevance in Diabetes Mellitus. *Molecules* **2022**, *27*, No. 155.
(50) Lo Piparo, E.; Scheib, H.; Frei, N.; Williamson, G.; Grigorov, M.; Chou, C. J. Flavonoids for controlling starch digestion: structural requirements for inhibiting human α-amylase. *J. Med. Chem.* **2008**, *51*, 3555−3561.
(51) Hawash, M.; Jaradat, N.; Shekfeh, S.; Abualhasan, M.; Eid, A. M.; Issa, L. Molecular docking, chemo-informatic properties, alpha-amylase, and lipase inhibition studies of benzodioxol derivatives. *BMC Chem.* **2021**, *15*, No. 40.

https://doi.org/10.1021/acsomega.3c00265
ACS Omega 2023, 8, 11433−11446